

# Nonclassical light in the presence of noise

kumulative Habilitationsschrift

zur Erlangung des akademischen Grades

*doctor rerum naturalium habilitatus (Dr. rer. nat. habil.)*

der Mathematisch-Naturwissenschaftlichen Fakultät

der Universität Rostock

vorgelegt von Dr. rer. nat. Andrii Semenov  
geboren am 1. Februar, 1972 in Kiew

eingereicht Rostock, 19. Januar, 2018

verteidigt Rostock, 2. Juli, 2018



**Dekan**

Prof. Dr. Klaus Neymeyr  
Mathematisch-Naturwissenschaftliche Fakultät  
Universität Rostock  
Wismarsche Straße 45  
18057 Rostock

**Gutachter**

Prof. Dr. Werner Vogel  
Institut für Physik  
Universität Rostock

Prof. Dr. Luis Lorenzo Sánchez-Soto  
Departamento de Optica  
Facultad de Fisica  
Universidad Complutense  
Madrid, Spain

Prof. Dr. Peter van Loock  
Institut für Physik  
Johannes Gutenberg-Universität  
Mainz

Prof. Dr. Bohdan Lev  
Bogolyubov Institute for Theoretical Physics  
National Academy of Sciences of Ukraine  
Kiev, Ukraine



## Acknowledgement

I would like to thank all my colleagues and friends with whom I have collaborated during my work with this thesis. Without discussions and support, which I got from my colleagues, this thesis would be impossible. Particularly, I would like to thank Werner Vogel (Universität Rostock) for supporting me during the years of my work in Rostock as well as for knowledge and a charge of optimism, which I get collaborating with him. Many important results in this thesis would be impossible without collaboration with Werner Vogel, Dmytro Vasyliev (Universität Rostock), Martin Bohmann (Universität Rostock), and Jan Sperling (University of Oxford, UK) as well as without enlightening discussions with Olexander Chumak (Institute of Physics, NASU, Ukraine). I very much appreciate discussions with my colleagues, particularly Boris Hage (Universität Rostock), Alexander Szameit (Universität Rostock), Bohdan Lev (BITP, NASU, Ukraine), which help me to understand better the theoretical and experimental backgrounds of quantum physics. I also thank Stefan Gerke (Universität Rostock), Martin Bohmann, Werner Vogel, and Jan Sperling for proofreading my thesis. Last but not least, I am extremely obliged to my family—my wife Natalia and my children Kateryna and Maxim for their patience, understanding, and support.



## **Selbstständigkeitserklärung**

Hiermit erkläre ich an Eides statt, dass ich die hier vorliegende Habilitationsschrift selbstständig und ohne fremde Hilfe verfasst habe, bis auf die in der Bibliographie angegebenen Quellen keine weiteren Quellen benutzt habe und die den Quellen wörtlich oder inhaltlich entnommene Stellen als solche kenntlich gemacht habe.

Andrii Semenov  
Rostock, 19. Januar, 2018.





# Contents

<b>Habilitation thesis</b>	<b>9</b>
Abstract . . . . .	9
1 Introduction . . . . .	10
1.1 Classical and quantum information . . . . .	10
1.2 Nonclassicality and phase-space functions . . . . .	11
1.3 Bell nonlocality . . . . .	15
1.4 Entangled states . . . . .	16
1.5 Coupling light modes with the environment . . . . .	17
1.6 Local sampling of phase-space functions . . . . .	18
1.7 Outline . . . . .	18
2 Cavities with unwanted losses . . . . .	19
2.1 State of the art . . . . .	19
2.2 Complete model of unwanted noise . . . . .	20
2.3 Noise-induced mode coupling . . . . .	21
2.4 Quantum-state extraction from the cavity . . . . .	23
2.5 Quantum endoscopy without atoms . . . . .	23
2.6 Reconstruction of cavity parameters . . . . .	24
2.7 Summary . . . . .	25
3 Imperfect photodetection . . . . .	26
3.1 State of the art . . . . .	26
3.2 Dark counts and stray light . . . . .	27
3.3 Reconstruction of photon-number statistics . . . . .	29
3.4 Beating the Tsirelson bound . . . . .	30
3.5 Geometrical model of photocounting . . . . .	31
3.6 Summary . . . . .	32
4 Quantum channels in the turbulent atmosphere . . . . .	34
4.1 State of the art . . . . .	34
4.2 Fluctuating-loss channels . . . . .	35
4.3 Probability distribution of the transmittance . . . . .	35
4.4 Bell nonlocality in atmospheric channels . . . . .	38
4.5 Transmitting quadrature squeezing . . . . .	40
4.6 Gaussian entanglement in the atmospheric channels . . . . .	42
4.7 Higher-order nonclassical effects . . . . .	44
4.8 Summary . . . . .	45
5 Conclusions . . . . .	46
Bibliography . . . . .	49
<b>Publications</b>	<b>66</b>
List of Publications . . . . .	66

# Habilitation thesis

## Abstract

Quantum physics is one of the most profound achievements of the twentieth century, which predetermined the technological progress of our time. Its fundamental backgrounds can be tested with presently available experimental techniques. These experiments open exciting perspectives for developing entirely new information technologies related to secure data transfer and extremely powerful computation. Nonclassicality, i.e. the impossibility to describe an observed phenomenon with principles of classical physics, is a resource for quantum communications and quantum computations.

Many nonclassical phenomena appear to be fragile against interactions of quantum system with an environment, which manifests itself in distinct, unavoidable noise. For practical purposes of quantum communications, one often uses nonclassical light as a carrier of quantum information. In this thesis I summarize my research at the Universität Rostock and at the National Academy of Sciences of Ukraine related to the impact of the environment during generation, propagation, and detection of nonclassical light. First, I will analyse unwanted effects in light sources, which are implemented with leaky cavities. Second, I will consider effects of imperfect photodetection. Third, I will present our theoretical consideration of free-space channels, which is the first self-consistent quantum-optical model involving the atmospheric turbulence.

## Zusammenfassung

Quantenphysik ist eine der tiefgreifendsten Errungenschaften des zwanzigsten Jahrhunderts, welche den technologischen Fortschritt in unserer Zeit geprägt hat. Ihre fundamentalen Grundlagen können mit heutigen experimentellen Technologien getestet werden. Diese Experimente eröffnen aufregende Perspektiven für die Entwicklung prinzipiell neuer Informationstechnologien bezüglich sicherem Datentransfer und extrem starker Rechenkapazität. Nichtklassizität, d.h. die Unmöglichkeit ein beobachtetes Phänomen mit den Gesetzen der klassischen Physik zu beschreiben, ist eine Ressource für Quantenkommunikation und Quantencomputer.

Viele nichtklassische Phänomene sind anfällig gegenüber Wechselwirkungen des Quantensystems mit einer Umgebung, was sich in ausgeprägten und unvermeidbaren Rauschen manifestiert. Für praktische Zwecke der Quantenkommunikation wird oft nichtklassisches Licht als Träger der Quanteninformation verwendet. In dieser Habilitationsschrift fasse ich meine Forschungsergebnisse an der Universität Rostock und der Nationalakademie der Wissenschaften der Ukraine bezüglich des Einflusses der Umgebung auf nichtklassisches Licht während der Erzeugung, der Ausbreitung und der Detektion zusammen. Zunächst, werde ich ungewollte Effekte in Lichtquellen analysieren, wobei der Fokus auf Resonatorquellen gelegt wird. Daraufhin, werde ich Effekte in nicht-idealer Photodetektion betrachten. Zuletzt, präsentiere ich unsere theoretische Beschreibung von Freiraumkanälen, die das erste selbstkonsistente quantenoptische Modell einschließlich atmosphärischer Turbulenz darstellt.

# 1 Introduction

My cumulative habilitation thesis is devoted to the consideration of effects of noisy environments on nonclassical properties of light. It includes a short review of twenty attached publications and one preprint with original research results. These papers and the preprint are listed on page 66 and referred in the text with Roman numerals. Other references are denoted by Arabic numerals.

In this chapter, I will briefly consider a general motivation of the research by giving special attention to applications in quantum communication. Particularly, I give a short introduction of the notion of nonclassicality and its connection to Bell non-locality and entanglement. I also consider why these phenomena can be regarded as a resource in quantum information and communication. I will give a short overview of the linear coupling of radiation fields with noisy environments and consider a procedure of local sampling of quantum phase-space distributions.

## 1.1 Classical and quantum information

The great technological leap forward occurring in the last decades is mostly related to the active development of information technologies. Today, these technologies are inherent tools of scientific, cultural, economical, governmental, and social activities as well as an important part of our everyday life. In this context, it is very important to understand the physical background, which lies behind the notion of information.

The mathematical fundamentals of information theory have first been proposed by Shannon [1, 2]. In physics, the notion of information is uniquely related to states of physical systems. The simplest systems used in quantum technologies have only two possible states, characterized by discrete values of a certain physical observable, usually referred to as bit. Another example is the state of a point-like particle, which is given by the position,  $q$ , and the momentum,  $p$ , or, equivalently, by a complex number  $\alpha = \frac{1}{\sqrt{2}}(q + ip)$ . The same mathematical structure is inherent to a description of an electromagnetic-radiation mode, see, e.g. [3, 4]. In this case  $q$  and  $p$  are physical observables known as mode quadratures and  $\alpha$  is the field-mode amplitude. Here, a complex value  $\alpha$  encodes a particular message.

The quality of information is typically characterized by an uncertainty. In this case, states of the system are characterized by probability distributions,  $\varrho(\alpha) \equiv \varrho(q, p)$ . In classical physics this uncertainty is caused only by the lack of our knowledge. Such states are usually referred to as mixed classical states. For the pure classical states, the value of  $\alpha$  is well defined.

Pure quantum states cannot be characterized by points in phase space. Instead, such a state is described by a vector  $|\psi\rangle$  in the Hilbert space of states, or equivalently by the density operator  $\hat{\varrho} = |\psi\rangle\langle\psi|$ . After interactions with the environment, the quantum state cannot be described by a single Hilbert-space vector. Instead, it can still be described by a density operator [5, 6] as  $\hat{\varrho} = \sum_n p_n |\psi_n\rangle\langle\psi_n|$ , where  $|\psi_n\rangle$  are certain orthogonal vectors in the Hilbert space, and  $p_n$  satisfies the conditions  $\sum_n p_n = 1$ ,  $p_n \geq 0$ . The evolution of the pure state into the mixed state is known as the decoherence process [7].

A typical communication task usually consists of three stages. At the first stage, the sender prepares a state,  $\varrho_{\text{in}}(\alpha)$  in classical or  $\hat{\varrho}_{\text{in}}$  in quantum communication. At the second stage, the state is transferred via a communication channel, which typically modifies it by introducing more uncertainties,

$$\varrho_{\text{out}}(\alpha) = \mathcal{L}\varrho_{\text{in}}(\alpha) \quad \text{or} \quad \hat{\varrho}_{\text{out}} = \mathcal{L}\hat{\varrho}_{\text{in}}, \quad (1.1)$$

where  $\varrho_{\text{out}}(\alpha)$  ( $\hat{\varrho}_{\text{out}}$ ) is the output state obtained at the receiver,  $\mathcal{L}$  is the channel operator (superoperator in the quantum case), describing the influence of the channel on states of

the system. At the third stage, a certain observable is measured. The outcome of this measurement is presented by numbers  $A$  with the probabilities

$$P(A) = \int_{\mathbb{C}} d^2\alpha \varrho_{\text{out}}(\alpha) \Pi(A|\alpha) \quad \text{or} \quad P(A) = \text{Tr} \left( \hat{\varrho}_{\text{out}} \hat{\Pi}(A) \right), \quad (1.2)$$

where  $d^2\alpha = d(\text{Re } \alpha) d(\text{Im } \alpha)$ . In this relation,  $\{\Pi(A|\alpha), A \in \mathcal{I}\}$  [ $\{\hat{\Pi}(A), A \in \mathcal{I}\}$ ] is the set of functions [operators] forming the positive-valued measure (PVM) [positive operator-valued measure (POVM)] for the given measurement procedure [8, 9] with the set of outcome values  $\mathcal{I}$ . The classical PVM can be interpreted as a probability to get the outcome value  $A$  under condition that the field amplitude is  $\alpha$ . The PVM [the POVM] is the positive-definite function [operator], which satisfy the completeness relation,

$$\sum_{A \in \mathcal{I}} \Pi(A|\alpha) = 1 \quad \text{or} \quad \sum_{A \in \mathcal{I}} \hat{\Pi}(A) = \hat{1}, \quad (1.3)$$

where  $\hat{1}$  is the unity operator.

Cryptographic key distribution [10] is an important part of communications protocols. A typical realization of this task with the Rivest-Shamir-Adleman (RSA) algorithm [11] assumes the computational hardness of the integer factorization with classical algorithms. However, this problem can be resolved by quantum computers [12] with Shor's algorithm [13, 14]. Even a potential possibility of its implementation in the nearest future, results in serious problems for the secure data transfer.

Quantum physics proposes a solution to this problem. Quantum key distribution (QKD) protocols [15, 16] utilize fundamental quantum properties in order to realize key distribution. As a physical carrier of information, these protocols use electromagnetic radiation in the optical domain. Depending on the measured observables, which may attain discrete or continuous values, the QKD protocols can be subdivided in discrete-variable (DV) [17–27] and continuous-variable (CV) [28–39] encodings, respectively.

In this context, natural questions arise, which have both applied and fundamental aspects. From a practical point of view, it is important to know if we can use classical systems in order to realize quantum algorithm and protocols. From a more fundamental point of view, it is interesting to understand if there exists a more general classical theory, which can explain quantum phenomena.

We will consider nonclassicality as the impossibility to describe observable phenomena in the framework of classical theory. And this defines what we can consider as a resource of quantum information and communication. Indeed, if given phenomena, which we use for quantum algorithms and protocols, can be explained with a classical theory, we can find a classical system, which can solve the corresponding task. It is therefore important to understand how stable nonclassicality is at all three stages of the communication protocols.

## 1.2 Nonclassicality and phase-space functions

If we aim to understand whether the given phenomena can be explained with classical theory, we should first give a clear definition for the notions of classical and quantum theory. Moreover, for a proper comparison of both theories, they should be formulated in the same “language”. Traditionally, the classical theory is formulated in terms of space-phase functions; whereas the quantum theory is presented in terms of operators on the Hilbert space of states. This difference, however, can be avoided by the formulation of quantum physics in terms of phase-space functions. For a review see [40].

As it has been shown by Shirokov [41], non-commutativity of observables, also in the phase-space representation [42], is the only difference between quantum and classical theories. An important consequence of this statement is the fact that the space of states essentially differs in quantum and classical theories. Indeed, the phase-space distributions in

quantum theory may have negative values. This fact does not have any classical explanation and it even contradicts classical probability theory.

We can consider nonclassicality of states from the operational point of view. Let us suppose that the given observable depends on a parameter  $a$ . In this case, the classical variant of Eq. (1.2) can be rewritten as

$$P(A|a) = \int_{\mathbb{C}} d^2\alpha \varrho(\alpha) \Pi(A|a; \alpha), \quad (1.4)$$

where  $P(A|a)$  is the probability to get the value  $A$  of the measured observable under the condition that the value of the parameter is  $a$ ;  $\Pi(A|a; \alpha)$  is the classical (i.e. non-negative) conditional PVM, i.e. the probability to get the value  $A$  under conditions that the value of the parameter is  $a$  and the value of the field amplitude is  $\alpha$ . If the classical theory holds, the system of integral equations<sup>1</sup> for  $\varrho(\alpha)$ , which is given by Eq. (1.4), has at least one positive semi-definite solution. If the solution is unique, the corresponding measurement procedure is referred to as tomographically complete.

Let us consider typical tomographically-complete measurements, which are often used in quantum optics. The schemes of the measurements and the related classical PVM are presented in the first and second row of Table 1, respectively. The balanced homodyne detection (see for reviews [3, 4, 43]), enables us to measure the phase-dependent field quadrature [44–50],  $x(\varphi) = q \cos \varphi + p \sin \varphi = \frac{1}{\sqrt{2}} (\alpha e^{-i\varphi} + \alpha^* e^{i\varphi})$ . The tomographic completeness of this procedure [51] has been used for reconstruction of phase-space distributions,  $\varrho(\alpha)$ , [52]. As an example, we consider a so-called single-photon-added thermal state (SPATS). The reconstructed phase-space distribution in this case has clear negative values [53]. This fact cannot be explained by the classical theory and, as that, it shall be considered as a manifestation of nonclassicality. The reconstructed phase-space distribution is the Wigner function  $W(\alpha)$  [54].

It turns out that negative values of the Wigner function are sufficient but not necessary certifiers of nonclassicality. In order to show this, let us consider the procedure of unbalanced homodyne detection, see the second column of Table 1. If we take only the probability of no counts,  $P(n=0|\alpha_o)$ , the corresponding system of equations will still be tomographically complete, since Eq. (1.4) is the invertible Weierstrass transform [55] in this case. The reconstructed function for SPATS differs from the Wigner function obtained with the balanced homodyne detection. As it follows from the quantum theory of photodetection [56, 57], the reconstructed distribution is the Glauber-Sudarshan P function [58, 59].

A key property of the P function is the possibility to present the density operator in the form

$$\hat{\varrho} = \int_{\mathbb{C}} d^2\alpha P(\alpha) |\alpha\rangle \langle \alpha|, \quad (1.5)$$

where  $|\alpha\rangle$  is a coherent state [3, 56, 60]. Consequently, the non-positivity of P function can be interpreted as the impossibility to present the given quantum state as a statistical mixture of coherent states [3, 61]. Note, that highly-singular values of P functions require an application of special methods for the verification of nonclassicality [62–65]. This kind of nonclassicality is also a key resource [66] for boson-sampling [67, 68], which is a special type of non-universal quantum computing based on the photoncounting procedure.

Nonclassicality with respect to the P function has important manifestations for photoncounting experiments. A famous example is the sub-Poissonian statistics of photocounts. The Mandel Q parameter [56, 69],

$$Q = \frac{\langle \Delta n^2 \rangle}{\langle n \rangle} - 1, \quad (1.6)$$

---

<sup>1</sup>The system of linear algebraic equations in the case of discrete variables.

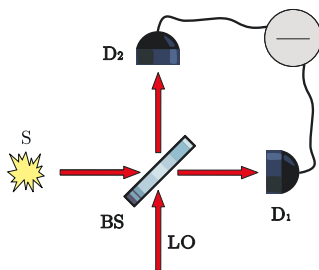
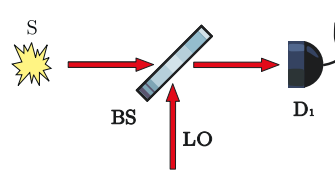
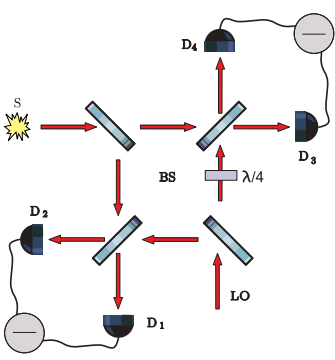
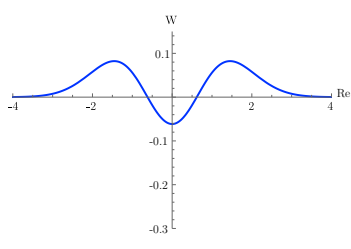
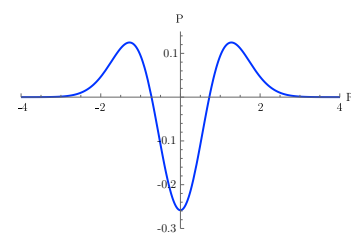
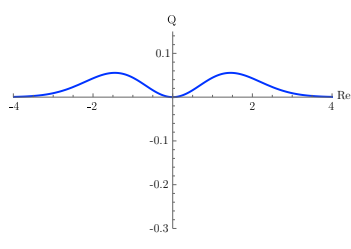
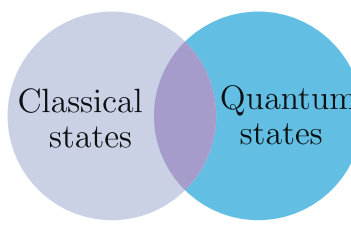
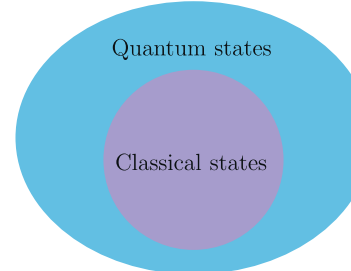
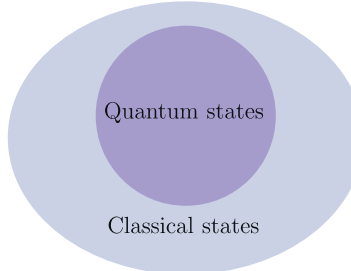
<p style="text-align: center;"><b>BHD</b></p> 	<p style="text-align: center;"><b>UHD</b></p> 	<p style="text-align: center;"><b>8HD</b></p> 
$\Pi(x \varphi; \alpha) = \delta\left(x - \frac{1}{\sqrt{2}}(\alpha e^{-i\varphi} + \alpha^* e^{i\varphi})\right)$	$\Pi(n \alpha; \alpha_o) = \frac{ \alpha - \alpha_o ^{2n}}{n!} \exp(- \alpha - \alpha_o ^2)$	$\Pi(\alpha_o \alpha) = \delta(\alpha_o - \alpha)$
<p style="text-align: center;"><b>Wigner function</b></p> 	<p style="text-align: center;"><b>P function</b></p> 	<p style="text-align: center;"><b>Q function</b></p> 
		

Table 1: The first row depicts different measurement schemes: balanced homodyne detection (BHD), unbalanced homodyne detection (UHD), and eight-port homodyne detection (8HD). Here BS are beam splitters (50:50 BS for BHD and 8HD, and large-transmittance BS for UHD), LO is the local oscillator (a laser signal of high [BHD and 8HD] and low [UHD] intensity), D and S are detectors and sources, respectively. The sign “−” denotes subtraction of photocurrents. The second row represents the corresponding classical PVM for quadratures, displaced photocounts, and field amplitude (from left to right). The third row illustrates the phase-space distributions (for  $\text{Im } \alpha = 0$ ) of a SPATS, reconstructed with the corresponding scheme. In quantum theory they correspond to the Wigner function, the P function, and the Q function, respectively. The last row shows relations between sets of classical and quantum states in the corresponding phase-space representations.

can be negative only when the corresponding P function is non-positive. In this case we deal with sub-shot noise measurements.

Therefore, operational nonclassicality of quantum states is a relative notion. It depends on the measurement procedure. For example, experimental results can be explained classically for a specific quantum state while operating with the balanced homodyne detection. For the same states, the results cannot have a classical explanation while operating with the unbalanced homodyne detection. In this context, it is interesting to note that the measurements with the procedure of eight-port homodyne detection [70] or heterodyne detection [8] have classical explanations in all cases, see the third column of Table 1. The quantum theory of this procedure (see e.g. [3, 43]) results to the conclusion that the reconstructed function is the Husimi-Kano Q function [71, 72], which is always non-negative.

An important consequence from the non-uniqueness of quantum-classical correspondence is that the relation between sets of quantum and classical states is also non-unique, see the last row of Table 1. For the Wigner representation, the sets of quantum and classical states have a certain intersection, where the Wigner functions are positive, cf., e.g., the Gaussian states [73]. Nonclassical states are the quantum states out of this domain. In this representation one can also consider non-quantum states, for example the pure classical state  $W(\alpha) = \delta(\alpha - \alpha_o)$ . These states, however, are not physical because the quantum theory represents a more general description of the Nature comparing with the classical theory. In the P representation, the set of classical states is completely included in the set of quantum states. The state  $P(\alpha) = \delta(\alpha - \alpha_o)$  is feasible in this representation and is, in fact, a coherent state. Nonclassical states in this case are all quantum states out of the classical domain. A completely opposite situation takes place for the Q representation. In this case, the set of quantum states is completely included in the set of classical states.

A very special role in this description is played by the phenomenon of quadrature squeezing [74–76]. Since the variance of quantum quadrature  $\langle \Delta \hat{q}^2 \rangle$  can be expressed in terms of the normal-ordered quadrature variance,  $\langle : \Delta \hat{q}^2 : \rangle$ , as

$$\langle \Delta \hat{q}^2 \rangle = \langle : \Delta \hat{q}^2 : \rangle + 1/2, \quad (1.7)$$

its value for the vacuum state is  $\langle \Delta \hat{q}^2 \rangle_{\text{vac}} = 1/2$ . The quadrature-squeezed states [77–79] have negative normal-ordered quadrature variance,  $\langle : \Delta \hat{q}^2 : \rangle < 0$ , because their P function is nonclassical. As that the quadrature variance of such states is less than the vacuum variance,  $\langle \Delta \hat{q}^2 \rangle < 1/2$ .

It is, however, important that the quadrature is measured with the balanced homodyne detection. Such a measurement is related to the Wigner function. The Wigner function of squeezed coherent states is positive. Hence, we can propose a classical theory, which explains quadrature squeezing. Of course, such a theory shall include a certain noise (so-called vacuum noise), whose nature is explained by quantum physics. Nevertheless, in the considered experiment this noise has completely classical characteristics.

Quadrature squeezing, however, is an important resource in quantum information. First, if we consider unbalanced homodyne detection or photocounting, the squeezed states will manifest nonclassicality. This can be used, e.g., in boson-sampling experiments [66]. Another application of the quadrature squeezing lies in a large group of CV QKD protocols [28, 33, 34, 38]. The main resource for these protocols, as well as for the coherent-state protocols [35, 36], is the Heisenberg uncertainty relation [80]  $\langle \Delta \hat{q}^2 \rangle \langle \Delta \hat{p}^2 \rangle \geq 1/4$ . The impossibility to violate this relation means that we cannot go outside the quantum domain (also in the classical domain outside its intersection with the quantum domain) in the Wigner representation. Therefore, for such protocols the main resource is quantumness rather than nonclassicality. With this example, it is clearly seen why it is important to distinguish between quantumness and nonclassicality.

### 1.3 Bell nonlocality

The operational nonclassicality considered in the previous subsection has a loophole. The problem is that the PVM  $\Pi(A|a; \alpha)$  depends on properties of the measurement device. Therefore, our conclusions depend on the corresponding knowledge. This leaves some loopholes for explaining the experimental results with classical theory. This feature also represents a security loophole for QKD protocols in the case when an eavesdropper may control the measurement device, i.e. the function  $\Pi(A|a; \alpha)$  [24, 25].

In order to overcome the problem, we have to exclude the information about the measurement device from Eq. (1.4). This can be done only in the case of a system with several degrees of freedom. Such a type of nonclassicality, which is known as Bell nonlocality [81], is better studied for discrete-variable systems.

We consider the following configuration of measurement, see Fig. 1.1. Two parties, Alice (A) and Bob (B), can measure observables,  $\sigma_A$  and  $\sigma_B$ , respectively. The observable  $\sigma_A$  ( $\sigma_B$ ) depends on the parameter  $\theta_A$  ( $\theta_B$ ), which in the considered scheme takes only two values  $\theta_A = \{\theta_A^{(1)}, \theta_A^{(2)}\}$  ( $\theta_B = \{\theta_B^{(1)}, \theta_B^{(2)}\}$ ). This means, that in the experiment, we can reconstruct the set of four probabilities  $P(\sigma_A^{(i)}, \sigma_B^{(j)} | \theta_A^{(i)}, \theta_B^{(j)})$ , which is usually referred to as the behaviour. We denote with  $\sigma_A^{(i)}$  ( $\sigma_B^{(i)}$ ) the value of the observable  $\sigma_A$  ( $\sigma_B$ ) when the value of parameter is  $\theta_A^{(i)}$  ( $\theta_B^{(i)}$ ). If the measurement result assumes a classical description, then such a probability distribution should exist,  $\varrho(\sigma_A^{(1)}, \sigma_A^{(2)}, \sigma_B^{(1)}, \sigma_B^{(2)} | \theta_A^{(1)}, \theta_A^{(2)}, \theta_B^{(1)}, \theta_B^{(2)}) \geq 0$ , for which the elements of the behaviour are marginal distributions, i.e.

$$P(\sigma_A^{(i)}, \sigma_B^{(j)} | \theta_A^{(i)}, \theta_B^{(j)}) = \sum_{\sigma_A^{(k)}, \sigma_B^{(l)}} \varrho(\sigma_A^{(1)}, \sigma_A^{(2)}, \sigma_B^{(1)}, \sigma_B^{(2)} | \theta_A^{(1)}, \theta_A^{(2)}, \theta_B^{(1)}, \theta_B^{(2)}), \quad k \neq i, l \neq j. \quad (1.8)$$

If such a function does not exist, the behaviour cannot be described with classical theories. It is very important that in contrast to Eq. (1.4), Eq. (1.8) does not depend on any characteristics of the measurement device.

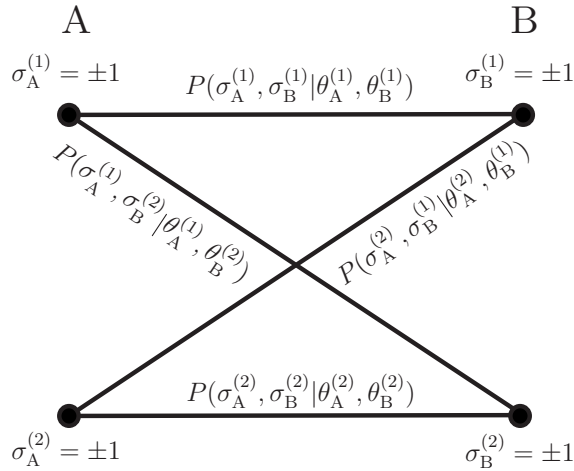


Figure 1.1: The standard scheme of Bell-nonlocality verification. See the text for more detailed explanations.

The Bell inequalities [82] in the Clauser-Horn-Shimony-Holt (CHSH) form [83] state a necessary and sufficient [84] condition for the existence of at least one positive semi-definite solution of the system of linear equations (1.8). If such a solution exists, the following in-



equalities are satisfied,

$$\mathcal{B} = \left| E\left(\theta_A^{(1)}, \theta_B^{(1)}\right) + nE\left(\theta_A^{(1)}, \theta_B^{(2)}\right) + mE\left(\theta_A^{(2)}, \theta_B^{(1)}\right) - nmE\left(\theta_A^{(2)}, \theta_B^{(2)}\right) \right| \leq 2, \quad (1.9)$$

where  $n, m = \pm 1$ , and

$$E\left(\theta_A^{(i)}, \theta_B^{(j)}\right) = \sum_{\sigma_A^{(i)}, \sigma_B^{(j)}} \sigma_A^{(i)} \sigma_B^{(j)} P\left(\sigma_A^{(i)}, \sigma_B^{(j)} | \theta_A^{(i)}, \theta_B^{(j)}\right) \quad (1.10)$$

is the correlation coefficient. Quantum physics can violate the CHSH inequalities. The maximal possible value in quantum theory, known as the Tsirelson bound [85], of the Bell parameter  $\mathcal{B}$  is  $\mathcal{B}_Q = 2\sqrt{2}$ . In the case, when at least one of the CHSH inequalities (1.9) is violated, the measurement result cannot be explained by the classical theories.

Since the measurements for Alice in Bob are assumed to be separated by a space-like interval, a very important question is whether quantum correlations do not violate the causality. This means that the measurement statistics of one party should not depend on the choice of another party [86]. Both classical and quantum correlations satisfy this non-signalling condition. It turns out that non-signalling correlations allow the violation of CHSH inequalities even beyond the Tsirelson bound up to the value,  $\mathcal{B}_{NS} = 4$ . Hence, quantum theory can be considered as a particular case of more general non-signalling theories. However, up to now, there is no experimental evidences about the post-quantum physics.

Bell nonlocality has been verified in many experiments. Let us mention just a few. The first violation of the CHSH inequalities has been verified by Freedman and Clauser in 1972 [87]. A disadvantage of that test was the fact that the settings of parameters  $\theta_A$  and  $\theta_B$  have been static. Aspect *et al.* have demonstrated for the first time in 1982 the Bell test with time-varying settings [88]. For the purposes of quantum communication it is important that violations of Bell inequalities have been demonstrated for long distances such as a 144km channel between the Canary Islands [89, 90] and a satellite-mediated 1200km channel over China [91].

Bell nonlocality is an important resource for QKD protocols. One of the first DV protocol, the Ekert protocol E91 [23], is based on checking the violations of Bell inequalities. Because Bell non-locality can be considered as a device-independent type of nonclassicality, the corresponding device-independent protocols have been considered in Refs. [24, 25].

## 1.4 Entangled states

The superposition principle is one of the most fundamental laws of quantum physics. Entanglement [92] is the manifestation of this property in the case of systems with two and more degrees of freedom. The first example of an entangled state has been considered in the famous paper by Einstein, Podolsky, and Rosen [93] for the demonstration of inconsistency, as it was suggested by the authors, of quantum theory. Werner has generalized the notion of entanglement to the case of mixed states [94].

There exist several different methods, which allow one to determine if a given state is entangled. For example, the separability-eigenvalue method [95] and the entanglement quasi-probability representation [96] proposed by Sperling and Vogel directly utilize the impossibility of presenting entangled states as a convex combination of separable states. There exists also a number of powerful sufficient conditions of entanglement, which can be used for analysis.

The Peres-Horodecki separability criterion [97–99] states that if the partial transpose of the density operator is not a positive semi-definite operator, then the state is entangled. The Shchukin-Vogel (SV) criterion [100] adapts this statement for the case of continuous-variable systems. If at least one minor of a specially-constructed matrix of moments is negative, then the state is entangled.

For our purposes it is important to consider only two of such minors, which result in the Simon [101] and Duan-Giedke-Cirac-Zoller (DGCZ) [102] criteria. According to these criteria a state is entangled if

$$\mathcal{W} = \det V^{\text{PT}} < 0, \quad (1.11)$$

where  $V^{\text{PT}}$  is the partial transposition of the matrix

$$V = \begin{pmatrix} \langle \Delta \hat{a}^\dagger \Delta \hat{a} \rangle & \langle \Delta \hat{a}^{\dagger 2} \rangle & \langle \Delta \hat{a}^\dagger \Delta \hat{b} \rangle & \langle \Delta \hat{a}^\dagger \Delta \hat{b}^\dagger \rangle \\ \langle \Delta \hat{a}^2 \rangle & \langle \Delta \hat{a} \Delta \hat{a}^\dagger \rangle & \langle \Delta \hat{a} \Delta \hat{b} \rangle & \langle \Delta \hat{a} \Delta \hat{b}^\dagger \rangle \\ \langle \Delta \hat{a} \Delta \hat{b}^\dagger \rangle & \langle \Delta \hat{a}^\dagger \Delta \hat{b}^\dagger \rangle & \langle \Delta \hat{b}^\dagger \Delta \hat{b} \rangle & \langle \Delta \hat{b}^{\dagger 2} \rangle \\ \langle \Delta \hat{a} \Delta \hat{b} \rangle & \langle \Delta \hat{a}^\dagger \Delta \hat{b} \rangle & \langle \Delta \hat{b}^2 \rangle & \langle \Delta \hat{b} \Delta \hat{b}^\dagger \rangle \end{pmatrix} \quad (1.12)$$

for the Simon criterion and the submatrix

$$V = \begin{pmatrix} \langle \Delta \hat{a}^\dagger \Delta \hat{a} \rangle & \langle \Delta \hat{a}^\dagger \Delta \hat{b} \rangle \\ \langle \Delta \hat{a} \Delta \hat{b}^\dagger \rangle & \langle \Delta \hat{b}^\dagger \Delta \hat{b} \rangle \end{pmatrix} \quad (1.13)$$

for the DGCZ criterion. Here  $\hat{a}$ , and  $\hat{b}$  are field annihilation operators for the mode associated with the party A and B, respectively. The Simon criterion is a necessary and sufficient condition for the entanglement of Gaussian states, i.e., for such states, which have a Gaussian Wigner function.

Gaussian entanglement is a resource for many quantum communication scenarios. For example, it is of importance for some CV QKD protocols (see, e.g. [38]), for CV teleportation [103], and for CV entanglement swapping [104]. It is also a resource for CV quantum computing [39, 105]. However, because the Wigner function of any Gaussian state is positive [106], nonclassical computing is impossible with homodyne detection only [107, 108]. To overcome this problem, one can use non-Gaussian states [109], photocounting measurements [110], or non-linear operations [105].

## 1.5 Coupling light modes with the environment

An interaction of quantum systems with an environment results in unavoidably diminishing nonclassical properties. In the case of relatively weak light fields, such as typically used in quantum information and communication, this interaction is reduced to linear coupling between light and environmental modes. The latter corresponds to scattering and absorption.

We consider a light mode, which is described by the field operator  $\hat{a}_{\text{in}}$  before interaction with an environment. We note that it can also represent a non-monochromatic mode, an intracavity mode at the initial moment of time, etc. This mode is coupled to the number of environmental modes, which can be combined in one effective environmental mode described by the operator  $\hat{c}$ . The linear character of coupling between light and environment modes yields the input-output relation,

$$\hat{a}_{\text{out}} = T \hat{a}_{\text{in}} + \sqrt{1 - |T|^2} \hat{c}. \quad (1.14)$$

Here  $\hat{a}_{\text{out}}$  is the field operator of the noisy light mode. The complex number  $T$ , which is referred to as the transmission coefficient, can be conveniently given in the form  $T = \sqrt{\eta} e^{i\varphi}$ , where  $\eta \leq 1$  is noted as the efficiency and  $\varphi$  represents the phase shift between output and input fields. In fact, Eq. (1.14) means that the considered noise effect can be described by a certain replacement scheme, which models the interaction by an effective beam splitter combining the light and the environmental mode.

The operator input-output relations (1.14) are easily transferred to the quantum-state input-output relations in the phase-space representation [3, 4]. In the optical domain the

state of environment can be considered as vacuum. This corresponds to losses (linear attenuation) of the light field. Particularly, for the P function the input-output relation reads

$$P_{\text{out}}(\alpha) = \frac{1}{|T|^2} P_{\text{in}}\left(\frac{\alpha}{T}\right). \quad (1.15)$$

This means that the attenuated state always preserves its nonclassicality with respect to the P function. For the Wigner function the input-output relation is given by

$$W_{\text{out}}(\alpha) = \int_{\mathbb{C}} d^2\beta W_{\text{in}}\left(\frac{\beta}{T}\right) \frac{1}{\pi|T|^2(1-|T|^2)} \exp\left(-\frac{2|\alpha-\beta|^2}{1-|T|^2}\right), \quad (1.16)$$

which adds Gaussian vacuum noise to the input state. The state, which is initially nonclassical with respect to the Wigner function, can lose the nonclassicality under linear attenuations.

## 1.6 Local sampling of phase-space functions

If the measurements, which are described by Eq. (1.4), are tomographically complete, the corresponding scheme can be used for the reconstruction of the density operator in the phase-space representation. For example, the balanced homodyne detection is used for the reconstruction of the Wigner function [51, 52]. Here, we briefly consider an alternative procedure for the local reconstruction of the Cahill-Glauber  $s$ -parametrized phase-space distributions [111, 112] proposed in [113, 114] and implemented in [115, 116].

The idea of local reconstruction is based on the fact that the  $s$ -parametrized phase-space distribution in the point  $\alpha$ ,  $P(\alpha; s)$ , is the mean value of the operator

$$\hat{P}(\alpha; s) = \frac{2}{\pi(1-s)} : \exp\left[-\frac{2}{1-s}\hat{n}(\alpha)\right] :, \quad (1.17)$$

where

$$\hat{n}(\alpha) = (\hat{a}^\dagger - \alpha^*)(\hat{a} - \alpha) \quad (1.18)$$

is the displaced photon-number operator [113]. The measurement of this observable can be performed with the unbalanced homodyne detection, see Table 1, first row, second column. With a small amount of loss, this procedure enables to get the measurement outcomes,  $n$ , of the observable (1.18). This renders it possible for us to reconstruct the corresponding displaced photon-number distributions,  $P_n(\alpha)$ , and to evaluate the needed mean value of the operator (1.18) with it.

## 1.7 Outline

In this cumulative habilitation thesis, I consider the effect of noise, based on the linear coupling between light modes and the environment, on nonclassical, non-local, and entanglement properties during the stages of generation, detection, and transmission of quantum states of light. In Chapter 2, we consider the role linear losses play in the cavity quantum electrodynamics (cavity QED). Imperfections of the photodetection, such as background radiation, dark counts, and impossibility to distinguish between adjacent photon numbers, is considered in Chapter 3. In Chapter 4, we study free-space channels and the effect of the turbulent atmosphere on the nonclassical light. The main conclusions of my research results are summarized in Chapter 5.

## 2 Cavities with unwanted losses

In this chapter I briefly review the main results obtained in my publications [I, II, III, IV, V, VI], in which we consider leaky cavities with unwanted noise, a necessary part of many sources of nonclassical light. In these publications I contributed in the following activities:

- Publication [I] – discussions of the main idea, analytical calculations, numerical simulations, discussions of the results;
- Publications [II, VI] – discussions of the main idea, analytical calculations, discussions of the results;
- Publications [III, IV] – discussions of the results;
- Publication [V] – part of analytical calculations, discussions of the results.

### 2.1 State of the art

A leaky cavity is a device which is a necessary part of many sources of nonclassical light. Besides the well-known fact that cavities are an important part of lasers [117], they are also used in optical parametric amplifiers for the generation of quadrature-squeezed light [3, 56, 74, 75, 118]. Another application of optical and microwave cavities in the framework of cavity QED is the manipulation of atoms inside cavities, for a review see, e.g., [119–121]. Particularly, they are used for quantum-state engineering of Schrödinger-cat states [122–128]. Quantum nondemolition measurements, first proposed in 1970's [129–131], are realized with atoms crossing a cavity [132–135]. Such a measurement reduces a quantum state of light to Fock states, which can also be used for the conditional generation of such states. Cavity QED enables also a preparation of Fock-states [136–139] and, in principle, any state on demand [140, 141]. There are also schemes for the generation of entangled states of different intracavity modes [142] and of ions in remote cavities [143, 144]. By using a special design of light pulses, one can consider the intriguing possibility of creating quantum networks with distant nodes [145].

Another important problem is quantum-state reconstruction of an intracavity mode. Two proposals have been discussed in the literature. The first one, the so-called quantum endoscopy method [146], probes the intracavity field by atoms. Another proposal [147] uses balanced homodyne detection for the reconstruction of the quantum state of a mode escaping from the leaky cavity.

Quantum noise theory [118, 148–150] (QNT) is the main theoretical tool in cavity QED. The radiation field in the framework of this approach is subdivided in an intracavity mode and the external field. We consider the case of a cavity without atoms, which is a good approximation in many cases of high-Q cavities for which the atom-transition time is much less than the decay time of the intracavity mode. In the Heisenberg picture, the field dynamic is described by the quantum Langevin equation,

$$\dot{\hat{a}}_{\text{cav}}(t) = -\left(i\omega_{\text{cav}} + \frac{\Gamma}{2}\right)\hat{a}_{\text{cav}}(t) + \sqrt{\Gamma}\hat{b}_{\text{in}}(t), \quad (2.1)$$

and the input-output relation,

$$\hat{b}_{\text{out}}(t) = \sqrt{\Gamma}\hat{a}_{\text{cav}}(t) - \hat{b}_{\text{in}}(t). \quad (2.2)$$

Here  $\hat{a}_{\text{cav}}(t)$  is the annihilation operator of the intracavity mode; the external field is described by the operators of input and output fields,  $\hat{b}_{\text{in}}(t)$  and  $\hat{b}_{\text{out}}(t)$ , respectively, which are defined here with respect to a certain phase. Such a cavity is defined by two parameters –  $\omega_{\text{cav}}$  is the frequency of the intracavity mode and  $\Gamma$  is the cavity decay rate.

Equations (2.1) and (2.2) are obtained in Refs. [118, 148–150] from a Hamiltonian which assumes a Markovian type of interaction between the intracavity mode and the external field. The phenomenological coefficients in this Hamiltonian can be derived from first principles [151, 152] by using the so-called Feshbach projection formalism [153]. Alternatively, Eqs. (2.1) and (2.2) are obtained directly from quantum field theoretical approaches [154–156].

The mentioned approaches do not consider the effect of unwanted losses caused by absorption and scattering. For high-Q cavities, such as considered, e.g., in Ref. [157], the amount of these losses can be rather small and the corresponding contribution may seem to be not significant. However, in such cavities unwanted losses are of the same order of magnitude as the wanted losses associated with the transmittance of the coupling mirror [158–160].

## 2.2 Complete model of unwanted noise

In this Section I will briefly discuss a generalization of quantum Langevin equation (2.1) and input-output relation (2.2) to the case of cavities with absorption and scattering proposed in Refs. [I, II, III, IV]. The first idea of how to treat unwanted losses in the quantum noise theory consists in modifications of the original Hamiltonian in Refs. [118, 148–150] by including the bath related to the absorption oscillators and scattering modes. Let us assume that only the intracavity field interacts with the bath. This results in a modification of the quantum Langevin equation (2.1),

$$\dot{\hat{a}}_{\text{cav}}(t) = -\left(i\omega_{\text{cav}} + \frac{\Gamma}{2}\right) \hat{a}_{\text{cav}}(t) + \mathcal{T}^{(c)} \hat{b}_{\text{in}}(t) + \mathcal{A}^{(c)} \hat{c}_{\text{in}}(t), \quad (2.3)$$

where  $\hat{c}_{\text{in}}(t)$  is the input-noise operator of the absorption/scattering system, and coefficients are related to each other as  $\Gamma = |\mathcal{T}^{(c)}|^2 + |\mathcal{A}^{(c)}|^2$ . In fact, the input-output relation resembles Eq. (2.2) in this case. Such a model is equivalent to the introduction of an additional input-output port for the cavity, such as it is done, e.g., for the two-sided cavity.

In realistic situations the absorption oscillators and the scattering fields also interact with the external field. This results in the appearance of noise terms not only for the quantum Langevin equation but also for the input-output relation. The complete model of a noisy cavity [I, II] is then described by the quantum Langevin equation

$$\dot{\hat{a}}_{\text{cav}} = -\left[i\omega_{\text{cav}} + \frac{1}{2}\Gamma\right] \hat{a}_{\text{cav}} + \mathcal{T}^{(c)} \hat{b}_{\text{in}}(t) + \hat{C}^{(c)}(t), \quad (2.4)$$

and the input–output relation

$$\hat{b}_{\text{out}}(t) = \mathcal{T}^{(o)} \hat{a}_{\text{cav}}(t) + \mathcal{R}^{(o)} \hat{b}_{\text{in}}(t) + \hat{C}^{(o)}(t). \quad (2.5)$$

Here, the complex coefficients  $\mathcal{T}^{(c)}$ ,  $\mathcal{T}^{(o)}$ , and  $\mathcal{R}^{(o)}$  characterize the injection of a pulse into the cavity, extraction from the cavity, and reflection from the cavity, respectively. The operators  $\hat{C}^{(c)}(t)$  and  $\hat{C}^{(o)}(t)$  satisfy the commutation rules,

$$[\hat{C}^{(c)}(t_1), \hat{C}^{(c)\dagger}(t_2)] = |\mathcal{A}^{(c)}|^2 \delta(t_1 - t_2), \quad (2.6)$$

$$[\hat{C}^{(o)}(t_1), \hat{C}^{(o)\dagger}(t_2)] = |\mathcal{A}^{(o)}|^2 \delta(t_1 - t_2), \quad (2.7)$$

$$[\hat{C}^{(c)}(t_1), \hat{C}^{(o)\dagger}(t_2)] = \Xi \delta(t_1 - t_2), \quad (2.8)$$

where  $\mathcal{A}^{(c)}$ ,  $\mathcal{A}^{(o)}$ , and  $\Xi$  are complex absorption/scattering coefficients.

The set of coefficients  $\omega_{\text{cav}}$ ,  $\Gamma$ ,  $\mathcal{T}^{(c)}$ ,  $\mathcal{T}^{(o)}$ ,  $\mathcal{R}^{(o)}$ ,  $\mathcal{A}^{(c)}$ ,  $\mathcal{A}^{(o)}$ , and  $\Xi$  characterizes leaky cavities with unwanted noise. However, the requirement of preserving the commutation rules, see [I, II], leads to the constraints for these coefficients,

$$\Gamma = |\mathcal{A}^{(c)}|^2 + |\mathcal{T}^{(c)}|^2, \quad |\mathcal{R}^{(o)}|^2 + |\mathcal{A}^{(o)}|^2 = 1, \quad \mathcal{T}^{(o)} + \mathcal{T}^{(c)*} \mathcal{R}^{(o)} + \Xi = 0. \quad (2.9)$$

These constraints define a manifold. Each realistic cavity is characterized by a certain point on this manifold.

As it has been analysed in Ref. [II], the commutation relations (2.6), (2.7), and (2.8) enable us to give a geometrical interpretation for the noise operators  $\hat{C}^{(c)}(t)$  and  $\hat{C}^{(o)}(t)$  as complex vectors. This means that there exists a basis  $\hat{c}_{\text{in}}^{(k)}$ , in which these vectors can be expanded,

$$\hat{C}^{(c)}(t) = \sum_{k=1}^n \mathcal{A}_{(k)}^{(c)} \hat{c}_{\text{in}}^{(k)}(t) \quad \text{and} \quad \hat{C}^{(o)}(t) = \sum_{k=1}^n \mathcal{A}_{(k)}^{(o)} \hat{c}_{\text{in}}^{(k)}(t), \quad (2.10)$$

where  $\mathcal{A}_{(k)}^{(c)}$  and  $\mathcal{A}_{(k)}^{(o)}$  play the role of the corresponding coordinates. The minimal dimensionality of this basis is  $n=2$ .

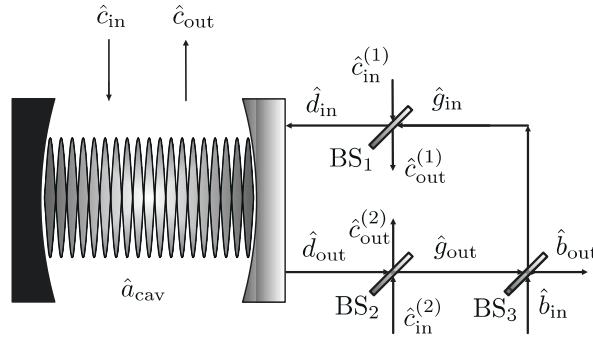


Figure 2.1: Complete and consistent replacement scheme, describing realistic cavities with unwanted noise.

It is also convenient to use the dimensionality  $n = 3$ . In this case, the unwanted noise can be modelled by internal cavity losses, by two beam splitters for the input and output ports, and by a beam splitter which models a feedback. The obtained replacement scheme, see Fig. 2.1, leads to the noise parameters in the form (2.10), with basis vectors  $\hat{c}_{\text{in}}$ ,  $\hat{c}_{\text{in}}^{(1)}$ , and  $\hat{c}_{\text{in}}^{(2)}$ , respectively. All parameters of the realistic cavity in this case are expressed in terms of beam-splitter parameters. This parametrization completely and consistently describes the manifold given by Eq. (2.9).

In Refs. [III, IV], we have used the methods of the quantum field theoretical approach [154] in order to derive the quantum Langevin equation and the input-output relation. As a result we have obtained Eqs. (2.4) and (2.5) from first principles. This confirms the validity of the proposed phenomenological result.

### 2.3 Noise-induced mode coupling

Here we briefly discuss the analysis of solutions of the quantum Langevin equation in Ref. [I]. We assume that the quantum state of the intracavity mode is generated at the zero point of time. The input and output fields can be expanded with orthonormal functions (pulses or nonmonochromatic modes),  $U_n^{\text{in(out)}}(t_1)$ , as

$$\hat{b}_{\text{in(out)}}(t_1) = \sum_{n=0}^{+\infty} U_n^{\text{in(out)}}(t_1) \hat{b}_{\text{in(out)};n}, \quad (2.11)$$

where  $\hat{b}_{\text{in(out)};n}$  are annihilation operators of an input (output) photon in the corresponding nonmonochromatic mode. For our purposes we choose the following nonmonochromatic

modes, see Fig. 2.2. First, we introduce the cavity-associated output mode (CAOM),

$$U_0^{\text{out}}(t_1) = \frac{F^*(t_1)}{\sqrt{\eta_{\text{ext}}}}, \quad \text{where} \quad F^*(t_1) = \mathcal{T}^{(o)} e^{-(i\omega_{\text{cav}} + \frac{\Gamma}{2})t_1} \Theta(t_1), \quad (2.12)$$

i.e. the output-field pulse in which the intracavity mode is extracted; here

$$\eta_{\text{ext}} = \int_{-\infty}^{+\infty} dt_1 |F(t_1)|^2 = \frac{|\mathcal{T}^{(o)}|^2}{\Gamma} \quad (2.13)$$

is interpreted as the extraction efficiency. Second, we present the matched input mode (MIM),

$$U_0^{\text{in}}(t_1) = U_0^{\text{out}}(t_1) e^{-i\varphi}, \quad (2.14)$$

which only contributes into the CAOM under the reflection from the cavity and differs from it by a certain phase  $\varphi$ . Third, we consider the additional output mode (AOM),

$$U_1^{\text{out}}(t_1) = \sqrt{\Gamma} e^{i\chi} (\Gamma t_1 - 1) e^{-(i\omega_{\text{cav}} + \frac{\Gamma}{2})t_1} \Theta(t_1), \quad (2.15)$$

in which the MIM is reflected additionally to the CAOM<sup>2</sup>. All other input and output modes are chosen to span the orthogonal completion of these modes.

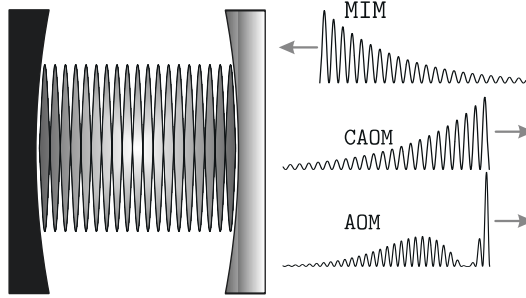


Figure 2.2: Nonmonochromatic modes of the external field: the cavity-associated output mode (CAOM), the additional output mode (AOM), and the matched input mode (MIM).

The input output relations for the considered modes are given by

$$\hat{b}_{\text{out};0} = \sqrt{\eta_{\text{ext}}} \hat{a}_{\text{cav}}(0) + \sqrt{\eta_{\text{ref}}} \hat{b}_{\text{in};0} + \hat{C}_0, \quad (2.16)$$

$$\hat{b}_{\text{out};1} = \sqrt{\eta_{\text{ref}}} \hat{b}_{\text{in};0} + \sum_{m=1}^{+\infty} G_{m,1}^* \hat{b}_{\text{in};m} + \hat{C}_1, \quad (2.17)$$

Here,

$$\eta_{\text{ref}} = \left| \frac{\mathcal{T}^{(o)} \mathcal{T}^{(c)}}{\Gamma} + \mathcal{R}^{(o)} \right|^2 \quad \text{and} \quad \bar{\eta}_{\text{ref}} = \frac{|\mathcal{T}^{(o)}|^2 |\mathcal{T}^{(c)}|^2}{\Gamma^2} \quad (2.18)$$

are the efficiency of the MIM reflection into the CAOM and the AOM, respectively.

Equation (2.16) describes the coupling of the intracavity mode and the input field in an output mode of the cavity. This effect is only possible if  $\eta_{\text{ref}} \neq 0$ . As it follows from Eq. (2.18), this efficiency is always zero for cavities, which do not have losses on absorption and scattering. Therefore, unwanted losses introduce a coupling between intracavity and input modes.

<sup>2</sup>See Ref. [1] for the explicit form of the phases  $\varphi$  and  $\chi$ .

## 2.4 Quantum-state extraction from the cavity

Let us consider a typical scenario of quantum-state extraction from the cavity, see Ref. [V]. A quantum state of the intracavity mode is generated at the zero time point. Then this mode leaks out of the cavity through the semitransparent mirror in the CAOM, and becomes available for further manipulations. In this case the input field is assumed to be in the vacuum state.

We rewrite Eq. (2.16) as

$$\hat{b}_{\text{out};0} = \sqrt{\eta_{\text{ext}}} \hat{a}_{\text{cav}}(0) + \sqrt{1 - \eta_{\text{ext}}} \hat{c}, \quad (2.19)$$

where  $\hat{c}$  combines the input field, scattering modes, and absorption oscillators being in the vacuum state. This equation completely resembles Eq. (1.14), which describes linear attenuation. Hence, input-output relations for the P function and the Wigner function between the intracavity mode and the CAOM are given by Eqs. (1.15) and (1.16), respectively, with  $T = \sqrt{\eta_{\text{ext}}}$ .

This means that the nonclassicality with respect to the P function will be preserved for all cavities. In other words, experiments involving unbalanced homodyne detection or photocounting may demonstrate results, which are impossible to explain in the framework of classical theory. However, the nonclassicality with respect to the Wigner function appears to be more fragile. This is why some experiments with nonclassical light in the cavity, which involve the balanced homodyne detection, can still be explained by a classical theory.

For example, the Wigner function of the single-photon state is always positive semi-definite for  $\eta_{\text{ext}} \leq 1/2$ . Because absorption/scattering losses are of the same order of magnitude as losses associated with the transmittance through the coupling mirror [158–160], the efficiency  $\eta_{\text{ext}}$ , see Eq. (2.13) together with Eq. (2.9), can be of order 1/2. Therefore, the nonclassicality for the Wigner function of the single-photon state is a hardly accessible task with presently available technologies.

## 2.5 Quantum endoscopy without atoms

The noise-induced mode coupling, which is described by Eq. (2.16), can be used for quantum-state reconstruction of the intracavity field. This proposal has been considered in Ref. [I]. We prepare the MIM in a coherent state and use it as a local oscillator for the intracavity mode. The CAOM in this case includes a combination of quantum states from the intracavity mode and the local oscillator. This can be used for quantum-state reconstruction with unbalanced homodyne detection [113, 114], see also Sec. 1.6.

The problem is that the reflected pulse also includes the AOM. In practice, it is difficult to filter out this mode, since the spectral characteristics of the CAOM and the AOM are very similar, see Ref. [I]. In order to overcome this problem, we propose to use the related scheme of cascaded homodyne detection [161] for local sampling of the Cahill-Glauber distribution. In this case, the balanced homodyne detection is used for the reconstruction of photon-number statistics [162, 163]. Therefore, the scheme of cascaded homodyne detection, see Fig. 2.3, includes two local oscillators. The first one, LO1, is prepared as the MIM. This pulse is reflected from the cavity. The second one, LO2, is prepared in the form of the CAOM. This local oscillator is phase randomized, i.e. it does not need a proper phase control. This form of the local oscillator in the balanced homodyne detection scheme enables one to completely exclude the influence of the AOM on the measured photon-number statistics.

The phase-space distribution of the intracavity mode,  $P_{\text{cav}}(\alpha; s)$ , is locally reconstructed as, cf. [161],

$$P_{\text{cav}}(\alpha; s) = \int_{-\infty}^{+\infty} dx S(x; s, \eta) p(x; \alpha), \quad (2.20)$$





At the first step, one uses the TP with  $\Gamma^{(k)}$  satisfying the condition  $\Gamma \ll \Gamma^{(k)} \ll \text{FSR}$ . In this case  $\eta_{\text{ref}}^{(k)} = |\mathcal{R}^{(o)}|^2$ . The phase of  $\mathcal{R}^{(o)}$  also corresponds to the phase of the total reflected pulse. Hence, by measuring the total efficiency of the reflection and the corresponding phase, we reconstruct the value of the cavity reflection coefficient  $\mathcal{R}^{(o)}$ .

At the second step, one measures two efficiencies,  $\eta_{\text{ref}}^{(k)}$ ,  $k = 1, 2$  for the TP's characterized by  $\Gamma^{(k)}$ . From this measurement we get the cavity-decay rate

$$\Gamma = \frac{\Gamma^{(2)} \left( \eta_{\text{ref}}^{(2)} - |\mathcal{R}^{(o)}|^2 \right) - \Gamma^{(1)} \left( \eta_{\text{ref}}^{(1)} - |\mathcal{R}^{(o)}|^2 \right)}{\eta_{\text{ref}}^{(1)} - \eta_{\text{ref}}^{(2)}}. \quad (2.23)$$

Also from the measurement results we evaluate another parameter

$$D = \Gamma \left( \Gamma + \Gamma^{(k)} \right) \left( \eta_{\text{ref}}^{(k)} - |\mathcal{R}^{(o)}|^2 \right), \quad (2.24)$$

which will be used in the next step.

At the third step, we apply the procedure of balanced homodyne detection with the local oscillator being in the CAOM in order to measure the efficiency of reflection into CAOM,  $\eta_{\text{ref}}^{(k)}$ . The cavity decay rate needed for the knowledge of the CAOM is supposed to be measured at the previous stage. Without loss of generality, we can consider  $\Gamma^{(k)} = \Gamma$ . This measurement enables us to reconstruct  $\mathcal{T}^{(o)}\mathcal{T}^{(c)}$ . Its absolute value is given by

$$|\mathcal{T}^{(o)}|^2 |\mathcal{T}^{(c)}|^2 = \frac{D}{2} + \Gamma^2 \left( |\mathcal{R}^{(o)}|^2 - \eta_{\text{ref}} \right), \quad (2.25)$$

and the phase

$$\arg \mathcal{T}^{(o)}\mathcal{T}^{(c)} = \arccos \frac{D - 4|\mathcal{T}^{(o)}|^2 |\mathcal{T}^{(c)}|^2}{4\Gamma |\mathcal{T}^{(o)}| |\mathcal{T}^{(c)}|} - \arg \mathcal{R}^{(o)}. \quad (2.26)$$

With the forth step of the measurement, we have to separate  $\mathcal{T}^{(o)}$  and  $\mathcal{T}^{(c)}$ . In general, it is impossible to do this with the reflection only. The value of  $\mathcal{T}^{(o)}$  can be obtained by measuring the efficiency and the corresponding phase for the pulse extracted from the cavity. This gives a possibility to evaluate also  $\mathcal{T}^{(c)}$  by using the value of  $\mathcal{T}^{(o)}\mathcal{T}^{(c)}$  evaluated at the previous step.

## 2.7 Summary

To summarize this section, we note that based on the quantum noise theory we provide the complete description for leaky cavities with unwanted noise. The obtained results are consistent with our parallel consideration of this problem in the framework of the quantum field theory approach. Particularly, we derived the quantum Langevin equation and the input-output relations describing such realistic cavities. The values of the cavity parameters are calculated from first principles via the quantum field theory approach. We also propose an operational procedure, which enables one to measure these parameters.

In many experimental situations the extraction of the quantum state of light generated in the cavity is important. We have shown that for high-Q cavities the efficiency of such an extraction can be of the order of 50%. This means that the extracted pulse always preserves the nonclassicality with respect to the P function. However, the nonclassicality with respect to the Wigner function will be lost in many experimental scenarios.

We have also considered the reflection of pulses from the cavity. From this consideration we have found that the coupling between the intracavity mode and the input pulse is only possible in the case of cavities with absorption/scattering losses. We proposed to use this effect for the local quantum-state reconstruction of the intracavity mode.

### 3 Imperfect photodetection

In this chapter, a brief review of my publications [VII, VIII, IX, X] and the preprint [XXI] is given. These works are devoted to the imperfect and noisy photodetection, which is an important measurement procedure in quantum optics. My contribution to these works consists in

- Publications [VII, X] – discussions of the main idea, analytical calculations, discussions of the results;
- Publication [VIII] – discussions of the main idea, discussions of methods, discussions of the results;
- Publication [IX] – discussions of the main idea, numerical simulations of data, discussions of numerical methods, analytical calculations, discussions of the results;
- Preprint [XXI] – discussions of the main idea, part of the analytical calculations, numerical simulations, discussions of the results.

#### 3.1 State of the art

Photoelectrical detection of light is a key measurement procedure, which is used in quantum-optical measurements. The quantum theory of photodetection [56, 57] states that the POVM [cf. Eq. (1.2) and the corresponding discussions] of counting  $n$  photons in the most ideal situation is a projector on the related Fock state,

$$\hat{\Pi}_n = |n\rangle \langle n| =: \frac{\hat{n}^n}{n!} \exp(-\hat{n}) :, \quad (3.1)$$

where  $\hat{n} = \hat{a}^\dagger \hat{a}$  is the photon-number operator and  $: \dots :$  denotes normal ordering. However, not all photons of the incoming radiation are counted by detectors. Some of them are missed for different reasons, for example, due to reflection of light from the detector surface. All these losses can be effectively modelled with a replacement scheme, which includes an effective beam splitter prior to an ideal detector. The field at the second port of the detector is assumed to be in the vacuum state. As a result the photodetection POVM reads

$$\hat{\Pi}_n =: \frac{(\eta \hat{n})^n}{n!} \exp(-\eta \hat{n}) :, \quad (3.2)$$

where  $\eta$  is the detection efficiency.

There exist several proposals for the compensation of losses in photodetection. The method of active compensation assumes preamplification of the signal [166, 167]. Another idea consists in numerical compensation of losses [168–170]. The corresponding methods require advanced mathematical techniques since this task is an example of the so-called ill-posed problems [171].

Another problem of photocounting detection is given by noise counts originating from the detector dark counts and stray light. Although a consistent theory of this phenomena for the classical light has been considered in 1969, cf. Refs. [172, 173], it was not adapted to the case of quantum light. In some later proposals, the model of dark counts with a single-mode thermal state at the second port of the effective beam splitter has been considered [174]. However, this theory is not in agreement with experiments since noise counts demonstrate clear Poissonian statistics, which significantly differs from the statistics of single-mode thermal states. An alternative suggestion uses phase-randomized coherent states in the second port of the effective beam splitter [175]. However, this idea leaves an open question about the physical backgrounds of such noise. To my best knowledge, only in Ref. [170] an ad-hoc quantum model of noise counts has been considered, which is consistent with experimental data and with earlier considerations for classical light in Refs. [172, 173].

In this chapter, I also refer to another problem of realistic photodetection. For most realistic detectors, it is hard to discriminate between adjacent photon numbers. Such on/off detectors may only distinguish between presence and absence of photons. If the source of light is weak enough, one may assume, that one click of the detector corresponds to one detected photon. This technique is applied for the realisation of the BB84 protocol [17] and similar single-photon QKD protocols, including the decoy-state protocol [21]. In such a case, one should apply special methods, so-called squash models [176–178], for correct mapping between infinite- and finite-dimensional Hilbert spaces related to the field mode and the measurement outcomes, respectively. A similar situation takes place for the realization of the E91 protocol [23] and other protocols based on checking the Bell inequalities including device-independent protocols [24, 25]. In practice, for checking the Bell inequalities, see e.g. [89, 90], one usually uses light pulses, which include more than one photon [179, 180].

In order to operate on/off detectors with light that contains more than one photon, different experimental techniques have been proposed. One of them assumes temporal [181–183] or spatial [184–187] splitting of light and then detecting each part with an on/off detector [188], see Fig. 3.1. The theory of such detectors has been formulated by Sperling, Vogel, and Agarwal [189]. See also [190–193] for more discussions about this theory. The number of clicks of such detectors, which are usually referred to as click detectors, is an observable value. This value can be described by the POVM

$$\hat{\Pi}_n = : \binom{N}{n} \left[ \hat{1} - \exp \left( -\frac{\hat{n}}{N} \right) \right]^n \exp \left( -\frac{\hat{n}}{N} \right)^{N-n} :, \quad (3.3)$$

where  $N$  is the number of on/off detectors in the array,  $n = \{0, N\}$  is the number of clicks. For this equation, we have assumed the unit efficiency and absence of dark counts.

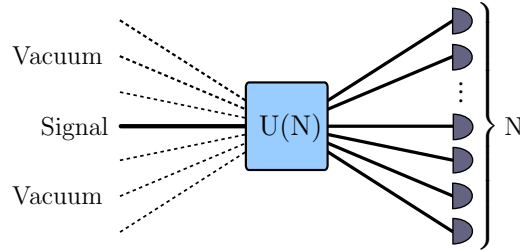


Figure 3.1: The scheme of click detectors. The initial signal is split in  $N$  beams, each of them is sent to the corresponding on/off detector.

A practical realization of local quantum-state reconstruction with unbalanced homodyne detection [113, 114], cf. also Sec. 1.6, requires very special conditions [115]. Two approaches to overcome this problem have been discussed in the literature. The first one proposes to reconstruct the click counterpart of the Cahill-Glauber distribution [194, 195]; see [196] for its experimental realization. Another approach [116] utilizes the technique of fitting of data patterns [197].

### 3.2 Dark counts and stray light

In this section, I will briefly present results of Ref. [VII], which also uses the results obtained in Ref. [VIII]. The main purpose of this consideration is to find the POVM of the photo-counting theory, which generalizes Eq. (3.2) to the case of non-zero noise counts. As it was mentioned above, the simple beam-splitter model with thermal or phase-randomized coherent noise [174, 175] yields no acceptable results.

Our idea is based on the observation reported in Refs. [56, 198, 199] that multimode thermal light is characterized by Poissonian statistics of photocounts. As that we assume

a multimode thermal noise at the second port of the effective beam splitter, see Fig. 3.2. Specifically, we suppose that the noise port is irradiated by  $\mu$  modes of thermal radiation each of them consists  $\nu/\mu$  thermal photons<sup>3</sup>. Only one thermal mode is considered to be interfered with the signal field; see Ref. [VII] for a more general case.

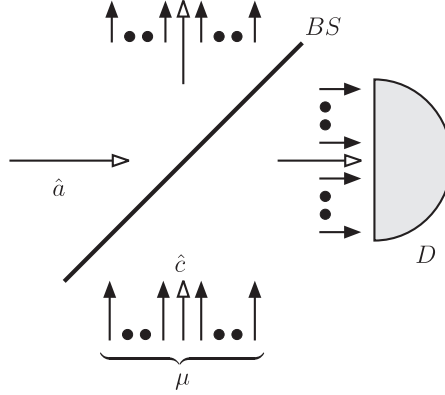


Figure 3.2: The model of a detector with losses and noise counts. Losses are modelled by a beam-splitter. However, the second port of the beam-splitter is irradiated by  $\mu$  modes of thermal light. One of these modes interferes with the signal.

Using the mathematical tool considered in Ref. [VIII], we have obtained the POVM for single-mode thermal noise. Including the rest of  $\mu - 1$  non-interfered modes in the obtained result, we get for the POVM of the detector

$$\hat{\Pi}_n = \frac{\left(\frac{\nu}{\mu}\right)^n}{\left(1 + \frac{\nu}{\mu}\right)^{n+\mu}} : \exp\left(-\frac{\eta}{1 + \frac{\nu}{\mu}} \hat{n}\right) L_n^{\mu-1}\left(-\frac{\eta}{\frac{\nu}{\mu} \left(1 + \frac{\nu}{\mu}\right)} \hat{n}\right) :, \quad (3.4)$$

where  $L_n^m(x)$  is the generalized Laguerre polynomial. The number of thermal modes can be approximately evaluated as  $\mu \approx \Delta\omega\tau$ , where  $\Delta\omega$  is the bandwidth of heat bath and  $\tau$  is the detection time. For the most practical applications in the optical domain,  $\mu$  is large such that  $\nu/\mu \ll 1$ . However, in the microwave domain this condition may not be satisfied.

In the limit  $\nu/\mu \rightarrow 0$ , the POVM (3.4) becomes

$$\hat{\Pi}_n =: \frac{(\eta\hat{n} + \nu)^n}{n!} \exp[-\eta\hat{n} - \nu] :. \quad (3.5)$$

The first important consequence of this equation is that the interference between signal and noise completely disappears. Hence, the noise counts represent an additive Poissonian noise. This fact was considered in Ref. [170] as an ad-hoc assumption. The parameter  $\nu$  is the mean number of noise counts during the detection time  $\tau$ , i.e. the intensity of noise counts. If we now apply the rule (1.2) to Eqs. (3.4) and (3.5) for a coherent state of light, we get the result obtained in Refs. [172, 173].

An interesting consequence of this consideration is the effect of noise counts on the sub-Poissonian statistics of photocounts. We consider the relation between the Mandel Q-parameters (1.6) without losses and noise,  $Q_{\text{in}}$ , and with them,  $Q_{\text{out}}$ ,

$$Q_{\text{out}} = \frac{\eta^2 \langle n \rangle}{\eta \langle n \rangle + \nu} Q_{\text{in}}. \quad (3.6)$$

It is clearly seen that the initially sub-Poissonian light with  $Q_{\text{in}} < 0$  is characterized by sub-Poissonian statistics of photocounts because in this case  $Q_{\text{out}} < 0$ . However, the amount of this negativity is diminished.

<sup>3</sup>For the sake of compatibility with other parts of the thesis, the notations differ from that in Ref. [VII].

### 3.3 Reconstruction of photon-number statistics

In Ref. [IX], we have presented a method, which enables one to compensate the effect of losses and noise in the measured photocounting statistics. We will distinguish between the photocounting statistics,  $\varrho_n$ , recorded by a detector with the efficiency  $\eta$  and noise-count intensity  $\nu$ , and the photon-number statistics,  $p_n$ , obtained with POVM (3.1), i.e. without losses and noise<sup>4</sup>. These probability distributions are related to each other as [VII, IX, 170]

$$\varrho_m = \sum_{n=0}^{+\infty} T_m^n p_n, \quad (3.7)$$

with

$$T_m^n = e^{-\nu} \nu^{m-n} \eta^n \frac{n!}{m!} L_n^{m-n} \left( \frac{\nu(\eta-1)}{\eta} \right) \quad (3.8)$$

for  $m \geq n$  and

$$T_m^n = e^{-\nu} (1-\eta)^{n-m} \eta^m L_m^{n-m} \left( \frac{\nu(\eta-1)}{\eta} \right) \quad (3.9)$$

for  $m \leq n$ .

Equation (3.7) can be analytically inverted [IX, 170], which gives a formal solution of the problem. However, this approach appears to be not practical since small experimental inaccuracies for the photocounting statistics,  $\varrho_n$ , result in large errors for the photon-number statistics,  $p_n$ . This equation represents a typical ill-posed problem [171].

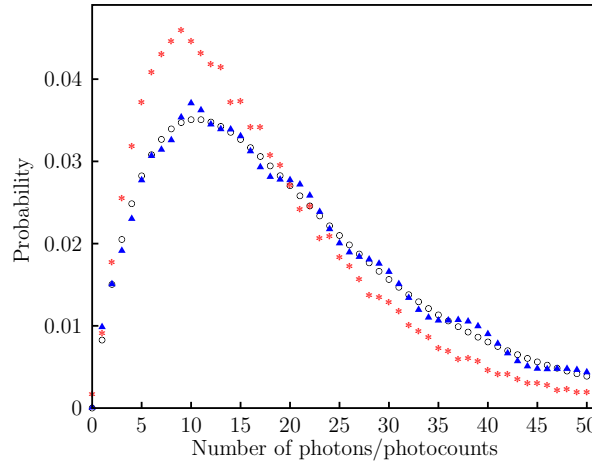


Figure 3.3: The numerically simulated photocounting statistics,  $\varrho_n$ , (asterisks) and the reconstructed photon-number statistics (triangles) of the SPATS are shown. The circles correspond to the theoretically-predicted photon-number statistics. For details see the text.

The regularization of the ill-posed problem consists in finding the minimum of the L2 discrepancy of Eq. (3.7) for the given  $\varrho_m$ , which satisfy some additional conditions including  $p_n \geq 0$ ,  $\sum_{n=0}^{+\infty} p_n = 1$ . This problem was resolved by us with the method of projected Landweber iterations [200–202]. The method demonstrate good results also for the case of imperfect knowledge of the matrix  $T_m^n$ , for example, when the efficiency,  $\eta$ , or noise-count intensity,  $\nu$ , are known with an error.

In order to check the method, we have performed numerical simulations. First, we simulate the photocounting statistics,  $\varrho_n$ , for some quantum states. Second, we apply the

<sup>4</sup>For the sake of compatibility with other parts of the thesis, the notations differ from that in Ref. [IX].

Landweber projected iterations by assuming an error for parameters  $\eta$  and  $\nu$ . The reconstructed photon-number statistics,  $p_n$ , is compared with the corresponding theoretically-predicted statistics.

The result for the example of a SPATS [53, 203] is shown in Fig. 3.3. We have used the state with the mean number of thermal photons  $\bar{n}_{\text{th}} = 10$ . The photocounting distribution,  $q_n$ , is simulated with  $5 \times 10^3$  sampling events for  $\eta = 0.7764$ ,  $\nu = 0.748$ . The photon-number distribution  $p_n$  is reconstructed with  $\tilde{\eta} = 0.77$ ,  $\tilde{\nu} = 0.75$ . This result is in a good agreement with the theoretically-predicted photon-number distribution.

### 3.4 Beating the Tsirelson bound

Here, we discuss an interesting consequence from the impossibility of detectors to distinguish between different adjacent photon numbers. This result is presented in Ref. [X]. We consider a typical scheme for testing Bell nonlocality, see Fig. 3.4. The source, S, irradiates photon pairs in a special polarization state. Each pair is analysed by Alice (A) and Bob (B) with polarization analysers. The polarisation analyser includes the half-wave plate (HWP), which rotates the polarization by an angle  $\theta_A$  ( $\theta_B$ ), polarization beam splitter (PBS), and two detectors  $D_{T_{A(B)}}$  and  $D_{R_{A(B)}}$ . For the given angle  $\theta_{A(B)}$  we associate the value of the corresponding observable  $\sigma_{A(B)} = +1$  if the photon registered by the detector  $D_{T_{A(B)}}$  and  $\sigma_{A(B)} = -1$  in the case of the detector  $D_{R_{A(B)}}$ . I refer to Sec. 1.3 for more details about the used notations. An important point is that we discard all other events such as no- and double-clicks at both detectors on one side.

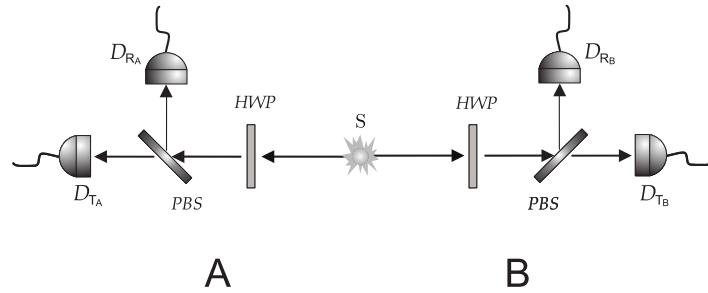


Figure 3.4: An experimental setup for checking the Bell nonlocality in optical experiments is shown. See the text for more details.

Let us consider the parametric down-conversion (PDC) source, which generates the state [179, 180]

$$|\Psi\rangle = (\cosh \xi)^{-2} \sum_{n=0}^{+\infty} \sqrt{n+1} \tanh^n \xi |\Phi_n\rangle, \quad (3.10)$$

where  $\xi$  is the squeezing parameter and

$$|\Phi_n\rangle = \frac{1}{\sqrt{n+1}} \sum_{m=0}^n (-1)^m |n-m\rangle_{H_A} |m\rangle_{V_A} |m\rangle_{H_B} |n-m\rangle_{V_B}. \quad (3.11)$$

The indices  $H_{A(B)}$  and  $V_{A(B)}$  correspond to the horizontally and vertically polarized modes, respectively. We have calculated the coefficients  $E(\theta_A, \theta_B)$ , cf. Eq. (1.10) taking into account that no- and double-click events are discarded. The result is substituted in the Bell parameter (1.9) for which we are looking for the maximal value with respect to the parameters  $\theta_A^{(1)}, \theta_A^{(2)}, \theta_B^{(1)}, \theta_B^{(2)}$ .

The result is presented in Fig. 3.5. Using on/off detectors we observe violations not only for the classical bound  $B = 2$  but also for the Tsirelson bound of quantum theory,

$\mathcal{B}_Q = 2\sqrt{2}$ . However, the result still does not beat the non-signalling bound,  $\mathcal{B}_{\text{NS}} = 4$ . The effect disappears when the detectors can distinguish between numbers of photons and we additionally discard all the events with more than one detected photon. This means that the violation of the Tsirelson bound is related to the impossibility of discriminating between different numbers of photons.

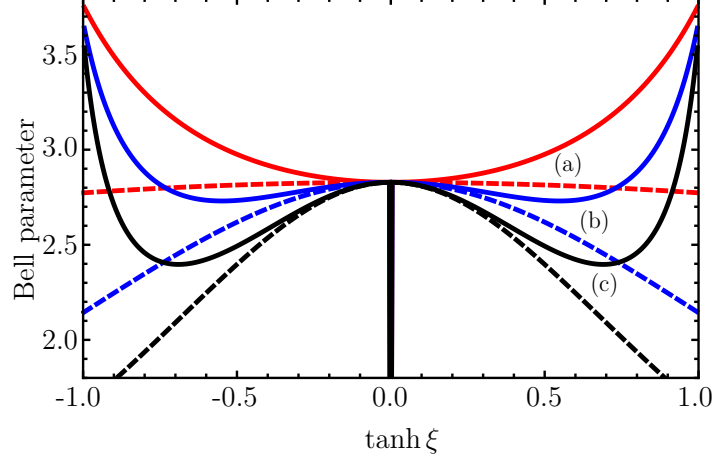


Figure 3.5: Maximal value of the Bell parameter,  $\mathcal{B}$ , for on-off (solid lines) and photon-number-resolving (dashed lines) detectors as the function of the squeezing parameter  $\tanh \xi$ . The noise-count intensity is  $\nu = 10^{-6}$ ; the detection efficiency is (a)  $\eta = 0.9$ , (b)  $\eta = 0.6$ , and (c)  $\eta = 0.4$ .

Of course, this result cannot be interpreted as witnessing the post-quantum physics because all calculations have been made in the framework of quantum theory. Similar effects have been discussed in the literature [204–206], and one of them has been experimentally tested [207]. We have discussed for the first time that this effect is observed with a typical scheme. The key point here is discarding the double-click events. Such a scenario leads to a security loophole when one applies it in QKD protocols. The above mentioned squash model [176–178] assumes that we should ascribe a random bit to each double-click event. In such a case the violation of the Tsirelson bound disappears.

### 3.5 Geometrical model of photocounting

In this section, I will give a brief review for the main results of Ref. [XXI]. We consider a method for the estimation of mean values of observables, which are functions of the photon-number operator,  $\hat{B} \equiv B(\hat{n})$ , based on measured data obtained from the click detectors. This result has many applications listed in [XXI]. One of them is the possibility to use click detectors for local quantum-state reconstruction with unbalanced homodyne detection [113–115], see also Sec. 1.6.

The main idea of the geometrical model of photocounting consists in the fact that the spectral resolution,

$$\hat{B} = \sum_{n=0}^{+\infty} B(n) |n\rangle \langle n|, \quad (3.12)$$

can be interpreted as the resolution of  $\hat{B}$  with respect to the basis  $|n\rangle \langle n|$ . The set of projectors  $|n\rangle \langle n|$  corresponds to the POVM for ideal photodetection, cf. Eq. (3.1). This basis is orthonormal with respect to the Hilbert-Schmidt (HS) scalar product, that is  $\text{Tr}(\hat{\Pi}_n \hat{\Pi}_m) = \delta_{nm}$ .



This is why the coefficients  $B(n) = B_n$  can be considered as coordinates of a vector associated with the operator  $\hat{B}$ .

The POVM of the click detectors (3.3) does not form such an orthonormal basis. Moreover, in the most general case it does not span the entire space of the considered class of observables. This means, that the resolution similar to Eq. (3.12) for this case is given by

$$\hat{B} = \sum_{n=0}^{N-1} B^n \hat{\Pi}_n + \hat{R}. \quad (3.13)$$

Here  $B^n$  is the so-called contravariant coordinate of the observable and  $\hat{R}$  is the orthogonal completion to the space spanned by the POVM (3.3). The term with  $n = N$  is excluded from the consideration since it can be uniquely expressed via other operators of POVM. As it is shown in Ref. [XXI], this term does not contribute to the sum.

The contravariant coordinates can be obtained by the standard methods of analytical geometry, see e.g. [208, 209]. For this purpose, we introduce the basis of the operators  $\hat{\Pi}^n$ , which form the contravariant operator-valued measure (COVM), such that

$$\text{Tr}(\hat{\Pi}^n \hat{\Pi}_m) = \delta_m^n. \quad (3.14)$$

The contravariant coordinates are given by

$$B^n = \text{Tr}(\hat{\Pi}^n \hat{B}). \quad (3.15)$$

By averaging over Eq. (3.13), we find the rule for evaluating the mean value  $\langle \hat{B} \rangle$ ,

$$\langle \hat{B} \rangle = \sum_{n=0}^{N-1} B^n \varrho_n + \langle \hat{R} \rangle, \quad (3.16)$$

where  $\varrho_n$  is the experimentally-reconstructed click-counting statistics and  $\langle \hat{R} \rangle$  is the systematic error. The rules for evaluating the latter are discussed in Ref. [XXI].

We apply this method for a local quantum-state reconstruction with unbalanced homodyne detection. After the displacement of the initial state by combining it with a weak local oscillator, we reconstruct the mean values of the operator  $\hat{P}(\alpha; s)$ , cf. Eq. (1.17) with the rule (3.16). Our estimation demonstrates that an acceptable result can be obtained even for small values of  $\alpha$  for some positive values of the parameter  $s$ , which is usually a hard task.

In order to test the method, we perform a numerical simulation. First, we simulate the displaced click statistics with  $10^5$  sampling events for a squeezed-vacuum state with the squeezing parameter  $\xi = 0.8$ . We assume a click detector with  $N = 8$ , the detection efficiency  $\eta = 0.7$ , and no dark counts,  $\nu = 0$ . Second, we use the simulated data for the reconstruction of the Wigner function ( $s = 0$ ) and the Cahill-Glauber distribution with  $s = 0.2$ . The results are shown in Fig. 3.6. From this simulation, we conclude that acceptable results are obtained for the Wigner function as well as for small values of  $\alpha$  for distributions with  $s > 0$ .

### 3.6 Summary

In this chapter, we considered realistic scenarios of photocounting as well as the effect of different inherent imperfections on nonclassical properties. First, we presented a consistent description of dark-count and stray-light noise. Our model of multimode thermal radiation explains the Poissonian statistics of noise counts and the additive character of the corresponding noise. We obtained the corresponding POVM, which includes the intensity of noise counts as an additional parameter. Also, we have found that noise counts can not destroy the sub-Poissonian character of the statistics completely. However, the amount of negativity

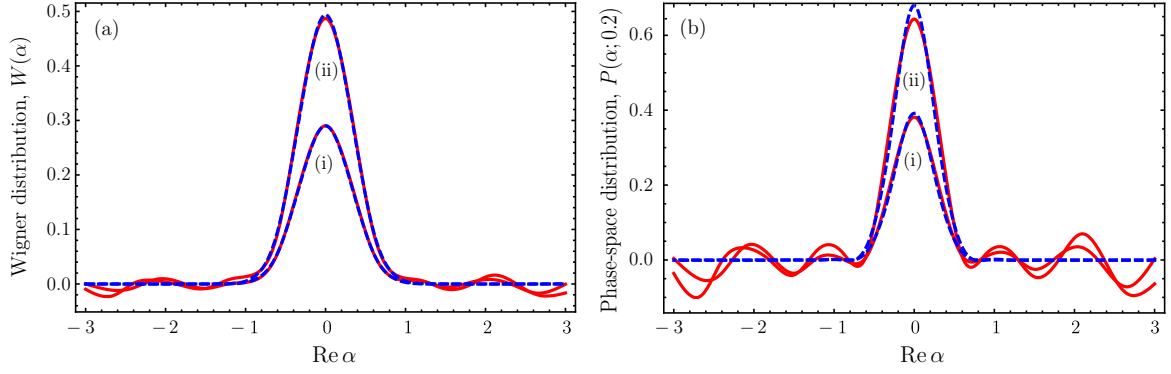


Figure 3.6: The theoretical (dashed lines) and reconstructed from the simulated data (solid lines) Cahill-Glauber phase-space distributions with (a)  $s = 0$  [Wigner function,  $W(\alpha)$ ] and (b)  $s = 0.2$  [the distribution  $P(\alpha; 0.2)$ ] for squeezed vacuum for (i)  $\text{Im } \alpha = 1$  and (ii)  $\text{Im } \alpha = 0$ .

of the Mandel  $Q$  parameter can be diminished. We have also considered a numerical technique, which enables one to reconstruct the photon-number statistics from lossy and noisy photocounting statistics.

Furthermore, we have studied the impossibility to discriminate between adjacent photon numbers. In optical tests of Bell nonlocality, this feature may result in surprising violations of Bell inequalities beyond the quantum Tsirelson bound. This phenomenon shall not be considered as a witnessing of post-quantum physics. The effect takes place only in the case of discarded double-click events. Such a discarding represents a security loophole while applying the Bell test for QKD protocols.

Finally, we also addressed the reconstruction of mean values of observables based on the data obtained from click detectors. This appears to be possible with the suggested procedure, which uses the basic analogy between quantum measurements and analytical geometry. We have applied this method to the local quantum-state reconstruction with unbalanced homodyne detection. Numerical simulations have demonstrated the applicability of the proposed technique also in the case of positive values of the Cahill-Glauber  $s$  parameter.

## 4 Quantum channels in the turbulent atmosphere

In this chapter I give a brief review of publications [XI,XII,XIII,XIV,XV,XVI,XVII,XVIII,XIX,XX], which are devoted to the quantum theory of the atmospheric communication channels. My contributions in these publications are

- Publications [XI, XVI] – discussions of the main idea, analytical calculations, discussions of the results;
- Publications [XII, XIV, XVIII, XIX] – discussions of the main idea, part of analytical calculations, discussions of the results;
- Publications [XIII, XV, XX] – discussions of the main idea, discussions of the results;
- Publication [XVII] – discussions of the main idea, part of numerical simulations, discussions of the results.

### 4.1 State of the art

Free-space quantum channels have a number of practical advantages for establishing quantum communication. First, one should note their flexibility — that means a possibility of the communication through hardly-accessible regions, in regions without fibre networks, and also with moving objects. Second, free-space channels open the intriguing perspective of establishing the satellite-mediated quantum communication, also on global scales. Moreover, free-space links can be used for other tasks such as improving global timekeeping systems [210] and interferometric telescopes [211]. They can also be applied for fundamental experiments, testing relativistic and gravitational effects in the quantum domain [212–214].

There exists a number of implementations, which demonstrate the feasibility of QKD protocols in free-space channels. Horizontal links have been tested for relatively short distances [215–220] as well as for long, more than 100km, channels [89, 90, 221–224]. In the last years an impressive progress in the satellite-mediated quantum communication [91, 225–236] has been achieved.

Atmospheric turbulence is the main disturbance factor for free-space channels. Classical optics of the turbulent atmosphere is a well-developed field of the research since the 1960's, see, e.g., Refs. [237–242]. Also, the classical-light propagation in the presence of haze, rain, and fog has been well studied [238, 243–251]. In earlier works [252–255], a model of log-normal intensity modulation for quantum light passing through the atmosphere has been proposed. Unfortunately, this theory exhibits some contradictions with fundamental laws of quantum physics. Its direct application may lead to unphysical results like creation of photons by the atmosphere [254]. Another approach proposed by Chumak *et al.* in Refs. [256–261] introduces a quantum distribution function of photons. This method satisfies all requirements of the quantum theory, and it appears to be especially useful for considering the effects for which the spatial or wave-vector structure of light modes is important.

The free-space QKD implementations can be subdivided in two big groups. One group includes QKD protocols, which use the spatial structure of optical modes by measuring, e.g., optical angular momentum [262]. This approach uses the spatial degrees of freedom of a radiation mode. It was demonstrated that this technique can also be practically applicable for free-space quantum communications [263–266].

In my habilitation thesis, I address another group of communication schemes, which use photocounting, homodyne detection, and polarization analysis. The idea of homodyne detection in atmospheric channels has been proposed and implemented in Refs. [267, 268]. Based on this idea quadrature squeezing has been transferred in a 1.6km channel [217]. Bell nonlocality has also been experimentally checked in a 144km channel [89, 90] and in a satellite-mediated 1200km channel [91]. The theoretical description of these experiments

as well as other ideas for quantum schemes in free-space channels are discussed in this chapter.

## 4.2 Fluctuating-loss channels

In this section, I will discuss the results of Ref. [XI]. To our best knowledge this is the first theoretical proposal which correctly describes quantum effects in the free-space channels. From the viewpoint of quantum-optical implementations, free-space links are linear lossy channels, which can be described with the methods presented in Sec. 1.5. An important feature of such channels is the fact that the transmission coefficient  $T$  is a random variable. This means that quantum-state input-output relation requires an additional averaging. For example, in the Glauber-Sudarshan  $P$  representation the input-output relation (1.15) is rewritten as

$$P_{\text{out}}(\alpha) = \int_{|T|^2 \leq 1} d^2T \mathcal{P}(T) \frac{1}{|T|^2} P_{\text{in}}\left(\frac{\alpha}{T}\right). \quad (4.1)$$

Here  $P_{\text{in/out}}(\alpha)$  is the  $P$  function of the input/output state and  $\mathcal{P}(T)$  is the probability distribution of the transmission coefficient (PDTC), which is the main characteristics of the atmospheric channel.

Equation (4.1) is the starting point for the research presented in this chapter. The analysis of quantum properties of light passing through such a fluctuating-loss channel is reduced to two main problems:

- Find an explicit form of the PDTC. According to the Ehrenfest theorem [269], the PDTC has the same form in classical and quantum optics. Hence, this problem can be resolved with the methods of classical optics.
- Analyse nonclassical (quantum) properties of the output state based on the given PDTC.

In the most of practical applications, one uses phase-insensitive measurements. Moreover, even the balanced homodyne detection can be designed in such a way, that the dephasing is negligible<sup>5</sup> [XVI, 267, 268]. This means that we can consider only the real transmission coefficient  $T = \sqrt{\eta}$ , where  $\eta$  is the transmission efficiency (transmittance). In this case, the input-output relation (4.1) is reduced to

$$P_{\text{out}}(\alpha) = \int_0^1 d\eta \mathcal{P}(\eta) \frac{1}{\eta} P_{\text{in}}\left(\frac{\alpha}{\sqrt{\eta}}\right), \quad (4.2)$$

where  $\mathcal{P}(\eta)$  is the probability distribution of the transmittance (PDT). Applying this equation to the photocounting problem of output light, one gets an equation, which resembles considerations in Refs. [252–255]. The difference is that the support of the corresponding probability distribution in those approach is  $\eta \in [0, +\infty)$ . The unphysical values of  $\eta > 1$  result in inconsistencies similar to creation of photons by the atmosphere [254].

## 4.3 Probability distribution of the transmittance

In this section, I will review the models of the PDT, which we proposed in Refs. [XII, XIII, XIV, XV]. As mentioned, this part of the problem is resolved by methods of classical optics. We consider a Gaussian beam transmitted through the atmosphere in the direction of the axis  $z$ . The atmospheric turbulence randomly destroys the initial beam shape and randomly

---

<sup>5</sup>Nevertheless, see Ref. [XI] for discussing the case of dephasing.

deviates the beam centroid. Only a part of the beam passes through the aperture at the receiver point  $z = L$ . The corresponding transmission efficiency reads as

$$\eta = \int_{\mathcal{A}} d^2\mathbf{r} I(\mathbf{r}; L), \quad (4.3)$$

where  $\mathcal{A}$  is the aperture area and  $I(\mathbf{r}; L)$  is the intensity normalized in the  $\mathbf{r} = \{x, y\}$  plane.

We assume that the effect of the atmosphere is reduced to the beam wandering and to random deformations of the beam in the elliptic form. With this assumption the intensity at the aperture plane is given by

$$I(\mathbf{r}; L) = \frac{2}{\pi \sqrt{\det \mathbf{S}}} \exp \left[ -2(\mathbf{r} - \mathbf{r}_0)^T \mathbf{S}^{-1} (\mathbf{r} - \mathbf{r}_0) \right], \quad (4.4)$$

with  $\mathbf{r} = (x \ y)^T$ . Here  $\mathbf{r}_0 = (x_0 \ y_0)^T$  are the coordinates of the beam centroid and the matrix  $\mathbf{S}$  characterizes the spot shape. This matrix is uniquely defined by the set  $\{W_1^2, W_2^2, \phi\}$ , where  $W_i^2$  are squared semiaxes of the ellipse and  $\phi$  is the angle between  $W_1$  and  $x$ .

By using the approximation method proposed in Refs. [XII, XIV] (see Ref. [XIII] for more mathematical details), we have been able to find an analytical approximation for the integral (4.3) after substituting the intensity (4.4). Therefore, the aperture transmittance can be considered as a function,  $\eta(\mathbf{v}, \phi)$ , of the random vector  $\mathbf{v} = (x_0 \ y_0 \ \Theta_1 \ \Theta_2)^T$  and the angle  $\phi$ . Here  $W_i^2 = W_0^2 \exp \Theta_i$  are parameters characterizing the beam shape, and  $W_0$  is the initial beam-spot radius. We assume that  $\phi$  is uniformly distributed. For the vector  $\mathbf{v}$  we assume the Gaussian distribution  $\rho_G(\mathbf{v}; \boldsymbol{\mu}, \Sigma)$  with the mean  $\boldsymbol{\mu}$  and the covariance matrix  $\Sigma$ . For the cases of weak-to-moderate and strong turbulences we have found the analytical expressions for  $\boldsymbol{\mu}$  and  $\Sigma$  by using the Huygens-Kirchhoff method and the Kolmogorov turbulence spectrum [270–273]. With such assumptions the PDT is given by [XIV]

$$\mathcal{P}(\eta) = \frac{2}{\pi} \int_{\mathbb{R}^4} d^4\mathbf{v} \int_0^{\pi/2} d\phi \rho_G(\mathbf{v}; \boldsymbol{\mu}, \Sigma) \delta[\eta - \eta(\mathbf{v}, \phi)]. \quad (4.5)$$

The integral in this expression can be numerically evaluated with a Monte Carlo method.

In the case when the beam does not change its shape, which happens for the weak turbulence, only beam wandering contributes to the PDT. In this case the integral in Eq. (4.5) can be analytically evaluated and the PDT is reduced to the log-negative Weibull distribution [XII],

$$\mathcal{P}(\eta) = \frac{R^2}{\sigma^2 \lambda \eta} \left( \ln \frac{\eta_o}{\eta} \right)^{\frac{2}{\lambda} - 1} \exp \left[ -\frac{1}{2\sigma^2} R^2 \left( \ln \frac{\eta_o}{\eta} \right)^{\frac{2}{\lambda}} \right], \quad (4.6)$$

for  $\eta \in [0, \eta_o]$ , and  $\mathcal{P}(\eta) = 0$  else. Here

$$\eta_o = 1 - \exp \left[ -2 \frac{a^2}{W^2} \right]. \quad (4.7)$$

is the maximal transmittance,  $a$  is the aperture radius,  $W^2 \equiv \langle W_{1,2}^2 \rangle$ , the parameters  $R$  and  $\lambda$  are certain functions of  $a$  and  $W$ , cf. Ref [XII], and  $\sigma^2$  is the beam-wandering variance. A similar consideration for the first two moments of the intensity of classical light has been investigated in Ref. [274].

In the case of weak-to-moderate turbulence, the PDT can be compared with the experimental data obtained in the 1.6km channel in the city of Erlangen [275], see Fig. 4.1(a). The data are fitted well with our elliptic-beam model and somewhat worse with the beam-wandering model. The truncated log-normal model is completely failing in this case.

As it has been demonstrated in the experiments over the 144km channel on the Canary Islands, see Ref. [223], the PDT in the case of strong-turbulence channels has a form that

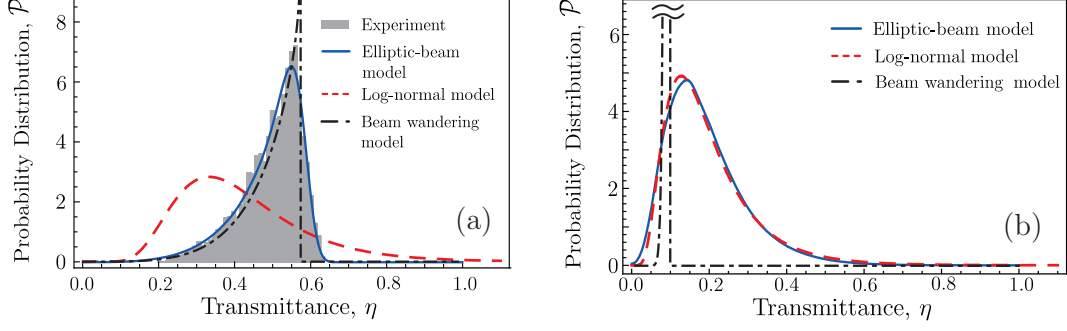


Figure 4.1: Different models of the PDT are shown: beam-wandering, elliptic-beam, and log-normal. (a): The case of weak-to-moderate turbulence for the 1.6km channel is compared with the experimental data (shaded area), see Ref. [275]. (b): The case of locally strong turbulence for the 2km channel is presented. See Ref. [XIV] for more details about the parameters.

resembles a truncated log-normal distribution. We consider a short-distance channel, which can still be described by the Kolmogorov turbulence spectrum, with strong local turbulence. Such conditions can be realized in a hot summer day. The corresponding PDT is shown in Fig. 4.1(b). The elliptic-beam PDT in this case is in a very good agreement with the truncated log-normal model. At the same time, the beam-wandering PDT shows a completely different behaviour.

Therefore, in the case of strong-turbulence channels, the PDT demonstrates a good agreement with the truncated log-normal model, which is given by

$$\mathcal{P}(\eta) = \frac{1}{\eta F(1) \sigma \sqrt{2\pi}} \exp \left[ -\frac{(\ln \eta + \mu)^2}{2\sigma^2} \right]. \quad (4.8)$$

Here  $F(x)$  is the cumulative probability distribution of the log-normal distribution. The parameters  $\sigma$  and  $\mu$  are related to the first two moments of  $\eta$  as

$$\sigma^2 \approx \ln \frac{\langle \eta^2 \rangle}{\langle \eta \rangle^2} \quad \text{and} \quad \mu \approx -\ln \left( \frac{\langle \eta \rangle^2}{\sqrt{\langle \eta^2 \rangle}} \right). \quad (4.9)$$

In turns, these moments are given by

$$\langle \eta \rangle = \int_{\mathcal{A}} d^2 \mathbf{r} \Gamma_2(\mathbf{r}; L) \quad \text{and} \quad \langle \eta^2 \rangle = \int_{\mathcal{A}} d^2 \mathbf{r}_1 \int_{\mathcal{A}} d^2 \mathbf{r}_2 \Gamma_4(\mathbf{r}_1, \mathbf{r}_2; L), \quad (4.10)$$

where  $\Gamma_2(\mathbf{r}; L) = \langle I(\mathbf{r}; L) \rangle$  and  $\Gamma_4(\mathbf{r}_1, \mathbf{r}_2; L) = \langle I(\mathbf{r}_1; L) I(\mathbf{r}_2; L) \rangle$  are the field correlation functions, which are evaluated by methods of classical atmospheric optics [238–242, 270–273]. These modifications of the standard log-normal distribution fix the problem in Refs. [252–255] such that the PDT (4.8) is applicable in the quantum domain.

Apart from geometrical losses related to the finite size of the receiver aperture, the light beam also suffers from the losses related to absorption and scattering. This is especially clear for diverse weather conditions when dust particles, aerosols, and precipitations play the role of random scatterers. These scatters also contribute to additional deformations of the beam shape. In the work [XV], which has been performed in collaboration with the experimental group from the Max Planck Institute for the Science of Light (Erlangen), led by Ch. Marquardt, we considered an extension of the elliptic-beam approximation for the case of rain and haze.

The results of our theory have been compared with experimental data obtained from measurements at the 1.6km-long channel in Erlangen. The measurements have been performed with rain of intensity 3.2mm/h and in the presence of haze. Both results have demonstrated a good agreement between the theory and the experimental data, see Fig. 4.2. Neither rain nor haze contributes to the beam wandering. In the case of low-intensity rain, contributions to the beam-shape deformations are minor and the main effect consists in additional deterministic losses. In the case of haze, contributions to the beam-shape deformations are significant.

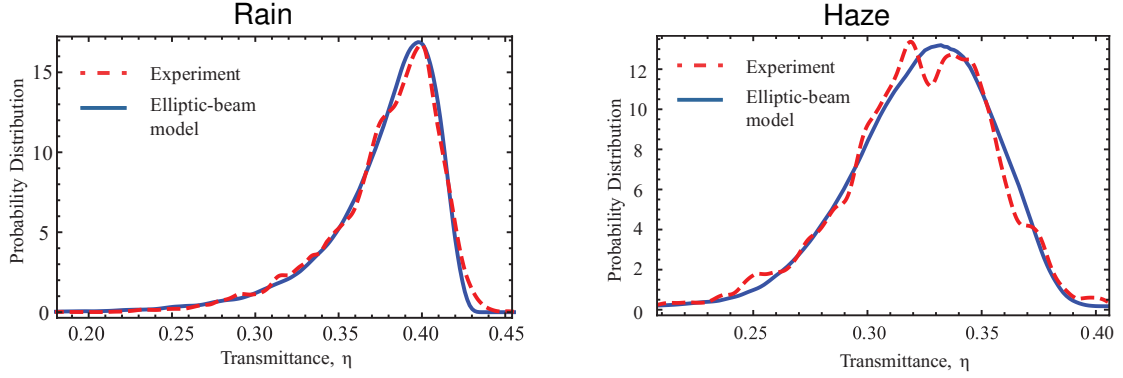


Figure 4.2: The theoretical and experimental PDTs in the case of low-intensity rain and haze. See the text and Ref. [228] for more details.

#### 4.4 Bell nonlocality in atmospheric channels

In this section, I will briefly recall our theoretical considerations of the Bell inequality test for light passing through the atmosphere, cf. [XVI, XVII]. The scheme of the experiment coincides with those discussed in Sec. 3.4, see also Fig. 3.4. However, the presence of the atmosphere between the source and the polarization analysers shall be taken into account.

Along with the channel losses, noise counts caused by detector dark-counts and stray light are serious disturbing factors for the considered experimental schemes. Indeed, such noise clicks can be counted instead of lost photons. Since noise counts represent an uncorrelated process, they significantly diminish the measured Bell parameter.

Additionally to a counterpropagation scheme, in which both modes propagate in different directions (channels), we also consider the copropagation scheme [90], which was implemented for the 144km channel on the Canary Islands, see Fig. 4.3. In this scheme both photons are sent in the same direction with a small delay interval, which is much smaller than the time for which the atmosphere is changed. This scheme includes a 50:50 beam splitter, which randomly selects the photons propagating to the receivers A and B. This beam splitter additionally introduces 3dB losses.

First, we consider the copropagation scheme. We will distinguish between the cases with discarding and incorporating double-click events, see the corresponding discussion in Sec. 3.4. Because the time interval between pulses of two modes is very small, one can consider that both channels to be correlated. Such channels may demonstrate violations of Bell inequalities much better than the deterministic-loss channels with the transmittance  $\eta_o$  equal to the mean transmittance of the considered channel,  $\langle \eta \rangle$ . This result can be explained by the fact that in such correlated channels the probability that photons in both channels reach the detector,  $\langle \eta^2 \rangle$ , as this probability,  $\eta_o^2$ , in the case of deterministic-loss channels. This fact is a consequence of the Cauchy-Schwarz inequality,  $\langle \eta^2 \rangle \geq \langle \eta \rangle^2$ . Indeed, in the case of strong turbulence, such as for the 144km channel, the Bell inequality can be violated in the case when the corresponding deterministic-loss channel does not demonstrate such

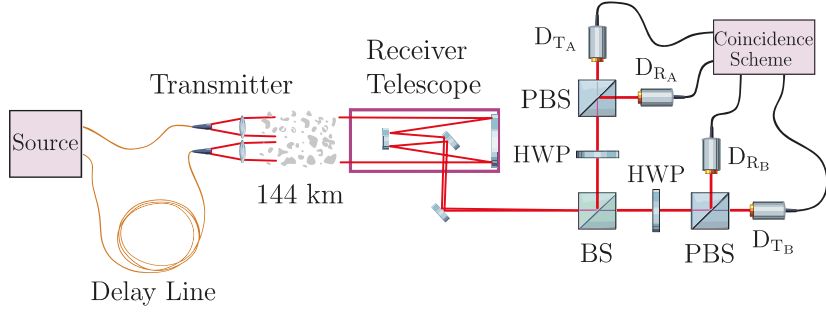


Figure 4.3: The copropagation scheme for checking the Bell inequalities as used in Ref. [90]. For more details, see the text.

violations, See Fig. 4.4(a). However, this effect disappears for the case of weak-to-moderate turbulence, such as in the 1.6km channel in Erlangen, see Fig. 4.4(b).

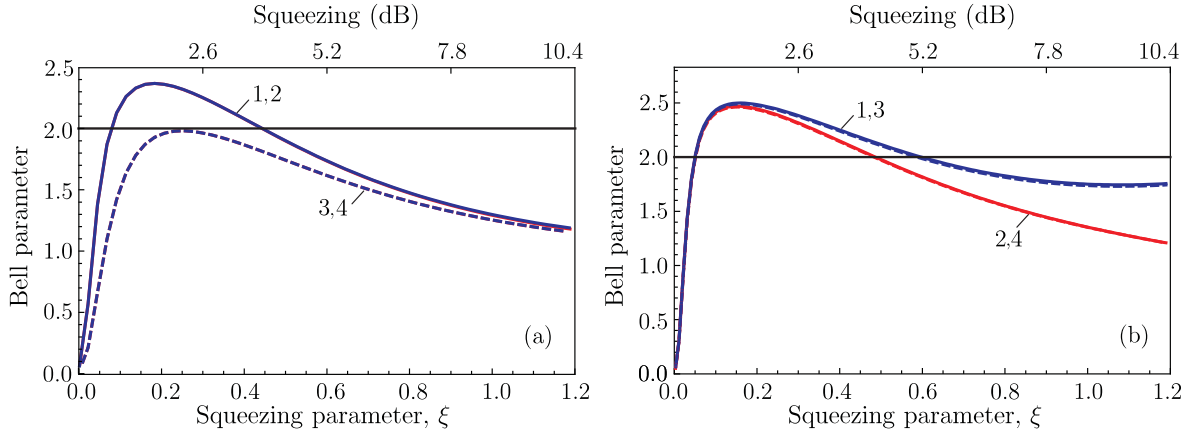


Figure 4.4: The Bell parameter,  $\mathcal{B}$ , vs the squeezing parameter,  $\xi$ , for the scenario of copropagation in the case of the PDC source generating the state (3.10). (a): The strong-turbulence 144km-long channel on the Canary Islands (the PDT is reconstructed from the experimental data in Ref. [223]), the noise-count intensity is  $\nu=1.7 \times 10^{-5}$ . (b): The weak to- moderate-turbulence 1.6km-long channel in Erlangen,  $\nu=3 \times 10^{-3}$ . The lines 1 and 2 correspond to fluctuating-loss channels without and with the incorporation of double-clicks events, respectively. The lines 3 and 4 correspond to the deterministic-loss channels with  $\eta_0 = \langle \eta \rangle$  without and with the incorporation of double-click events, respectively. For more details see Ref. [XVII].

In the scenario of counterpropagation, the advantages of fluctuating-loss channels completely disappears. However, in this case we can use a strategy similar to the one proposed in Ref. [223] for the decoy-state QKD protocol. For this purpose one sends intense light pulses before the weak pulses of the nonclassical light. With these pulses one can check the transmittance of the channel. We propose to postselect only such events, which have the transmittance in both channels exceeding a certain threshold value,  $\eta_{ps}$ . The feasibility of such a procedure is characterized by the probability that such events appear,

$$\overline{F}_{AB}(\eta_{ps}) = \overline{F}_A(\eta_{ps}) \overline{F}_B(\eta_{ps}), \quad \text{where} \quad \overline{F}_{A(B)}(\eta_{ps}) = \int_{\eta_{ps}}^1 d\eta \mathcal{P}_{A(B)}(\eta). \quad (4.11)$$

The results of the corresponding calculations are presented in Fig. 4.5. We have chosen the noise-count intensity such that the verification of Bell nonlocality is impossible. However, the



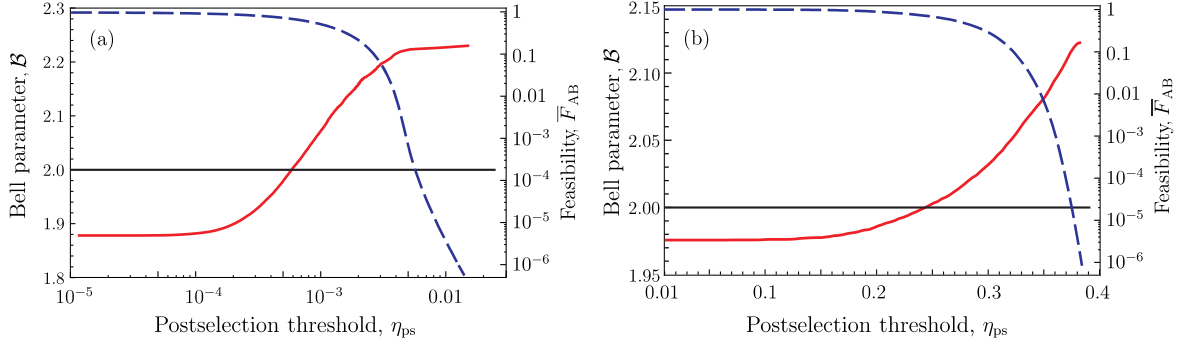


Figure 4.5: The Bell parameter,  $\mathcal{B}$ , vs the postselection efficiency,  $\eta_{ps}$ , (solid line) and the feasibility (4.11) of the postselection procedure,  $\bar{F}_{AB}$  (dashed line). (a): The strong-turbulence 144km-long channel on the Canary Islands; the noise-count intensity is  $\nu=4 \times 10^{-4}$ , the squeezing parameter  $\xi=0.25$ . (b): The weak to- moderate-turbulence 1.6km-long channel in Erlangen;  $\nu=2 \times 10^{-2}$ , the squeezing parameter is  $\xi=0.31$ . For more details see Ref. [XVII].

proposed postselection procedure improves the situation and violations of the Bell inequality become feasible.

#### 4.5 Transmitting quadrature squeezing

In order to test quadrature squeezing for light sent through the turbulent atmosphere, one has to realize balanced homodyne detection at the receiver station. For this purpose, one should synchronize the phases between the signal and the local oscillator. Moreover, the spatial structure of their modes shall also be identical. Usually, this is realized by originating the signal and the local oscillator from the same source. However, in the case of atmospheric channels, this experimental task is tricky enough since the atmosphere randomly changes both the phase and the spatial structure.

This problem has been experimentally resolved in Refs. [267, 268], see Fig. 4.6. The main idea utilizes the fact that the polarization effect of the atmosphere is negligibly small [237]. As that, one can send the signal and the local oscillator in the same spatial but orthogonally polarized modes. Experiments in Ref. [267] confirmed the absence of phase noise.

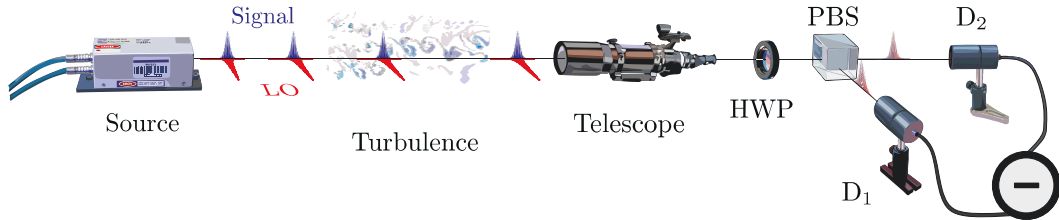


Figure 4.6: Scheme of homodyne detection for quantum light passing through the turbulent atmosphere as proposed in Ref. [267, 268]. The signal and the local oscillator are sent in the same spatial but orthogonally polarized modes. The half-wave plate (HWP) and the polarization beam-splitter (PBS) interfere the signal and the local oscillator. The output signals from the PBS are analysed at the detectors  $D_1$  and  $D_2$ .

In Ref. [XVIII] we provided a theoretical analysis of this scheme. As mentioned previously, the phase of the local oscillator is perfectly controlled. However, the amplitude contin-

uously fluctuates. It can be independently monitored by another detector or by adding the intensities at both detectors. We also assume a bright stray light of the intensity<sup>6</sup>  $\nu$ . Let  $\eta_m$  be the measured transmission efficiency, which can randomly differ from the actual transmittance  $\eta$ . In this case, the reconstructed output state will contain a certain postprocessing noise, which is caused by our imperfect knowledge of the atmosphere transmission. The P function of the noisy output state,  $P_{\text{out}}$ , is related to the P function at the transmitter,  $P_{\text{in}}$ , as

$$P_{\text{out}}(\alpha) = \int_0^1 d\eta \int_0^1 d\eta_m \mathcal{P}(\eta, \eta_m) \frac{\eta_m}{\eta^2} \exp \left[ \left( \frac{\eta - \eta_m}{8\eta_m} + \frac{\nu}{4r^2\eta_m^2} \right) \Delta_\alpha \right] P_{\text{in}} \left( \frac{\sqrt{\eta_m}}{\eta} \alpha \right), \quad (4.12)$$

where  $\mathcal{P}(\eta, \eta_m)$  is the joint PDT of the actual and measured transmittances,  $r$  is the amplitude of the local oscillator at the transmitter, and  $\Delta_\alpha = \frac{\partial^2}{\partial^2 \text{Re } \alpha} + \frac{\partial^2}{\partial^2 \text{Im } \alpha}$ . For simplicity, we consider a unit detection efficiency. The P function  $P_{\text{out}}$  may not correspond to a real physical state since it includes the postprocessing noise. This noise may even result in negative eigenvalues of the reconstructed density operator. This does not mean violations of quantum physics. This result is an artefact of our imperfect knowledge of the system parameters.

For the case of noiseless measurement of the transmittance,  $\mathcal{P}(\eta, \eta_m) = \mathcal{P}(\eta) \delta(\eta - \eta_m)$ , Eq. (4.12) is reduced to

$$P_{\text{out}}(\alpha) = \int_0^1 d\eta \mathcal{P}(\eta) \frac{1}{\eta} \exp \left[ \frac{\nu}{4r^2\eta^2} \Delta_\alpha \right] P \left( \frac{\alpha}{\sqrt{\eta}} \right). \quad (4.13)$$

From this equation, we conclude that very small values of the transmittance,  $\eta \ll r^2/\nu$ , may significantly destroy the nonclassical properties of output state. For this reason, one should always discard the events with very small transmittances in the presence of bright stray light. If the local oscillator is strong enough, Eq. (4.13) is reduced to the ordinary input-output relation in the fluctuating-loss channels, cf. Eq. (4.2).

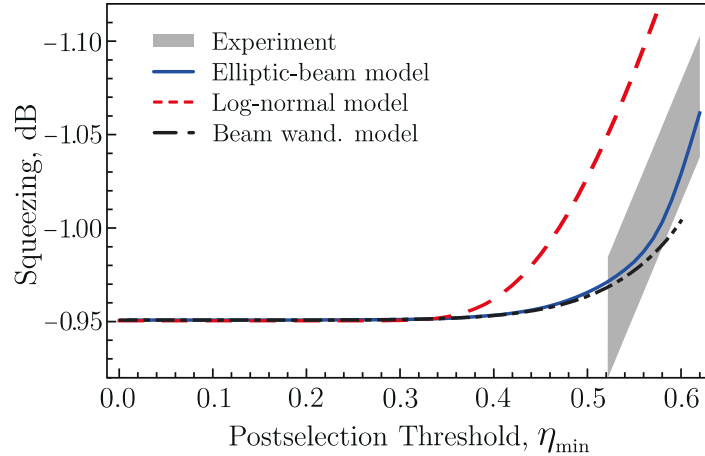


Figure 4.7: The value of squeezing in dB vs. the postselection threshold,  $\eta_{\text{min}}$ , obtained with different PDT models. The shaded area corresponds to the experimental data obtained in Ref. [217]. See Ref. [XIV] for more details.

The normal-ordered variance of the quadrature,  $\langle : \Delta \hat{q}^2 : \rangle$ , according to Eq. (1.7), can be considered as a certifier of quadrature squeezing. We apply input-output relation (4.2) in order to connect these variances at the input and output,

$$\langle : \Delta \hat{q}^2 : \rangle_{\text{out}} = \langle T^2 \rangle \langle : \Delta \hat{q}^2 : \rangle_{\text{in}} + \langle \Delta T^2 \rangle \langle \hat{q} \rangle_{\text{in}}^2, \quad (4.14)$$

<sup>6</sup>For the sake of compatibility, the notations differ from that in Ref. [XVIII].

where we remind that  $T = \sqrt{\eta}$ . The first term in this equation resembles the same for the deterministic-loss channels. The second term appears due to the effect of the atmospheric turbulence. It is clearly seen that the effect of turbulence disappears if the state is not displaced in the direction of the squeezed quadrature, i.e.  $\langle \hat{q} \rangle_{\text{in}} = 0$ .

The possibility of real-time monitoring of the channel transmittance can be used not only for discarding the stray-light effect but also for improving nonclassical/quantum effects, e.g. quadrature squeezing. For this purpose, one should postselect only the events with the transmittance exceeding a chosen postselection threshold  $\eta_{\text{min}}$ . The corresponding idea has been discussed in Ref. [XII]. It was experimentally implemented in the 1.6km channel in Erlangen [217]. In Fig. 4.7, we presented the results of the corresponding theoretical consideration for three models of the PDT, which are compared with the experimental data. One can clearly see a very good agreement between the experimental data and our elliptic-beam approximation.

#### 4.6 Gaussian entanglement in the atmospheric channels

The idea of analysing quadrature squeezing with the input-output relation for the corresponding certifier, cf. Eq. (4.14), can be clearly generalized to other nonclassical and quantum effects. For example, one can consider a similar input-output relation for the Simon certifier of Gaussian entanglement, cf. Eq. (1.11). Of course, after passing atmospheric channels, the initially Gaussian entangled state is not Gaussian in general. However, in many quantum CV protocols, only the Gaussian part of the state plays a role. For this reason, the certification of Gaussian entanglement is of substantial interest. After publishing Refs. [XII, XVIII], considerations of some particular scenarios of Gaussian entanglement have been presented [275, 276], in which the results of our works have been used. Our study in Ref. [XIX] introduces the complete analysis of this problem.

We assume that the measurement is performed with balanced homodyne detection. This gives us a possibility to use a two-mode variant of the quantum-state input-output relation (4.2). The channel associated with the party A(B) is characterized by the real transmission coefficient  $T_a = \sqrt{\eta_a}$  ( $T_b = \sqrt{\eta_b}$ ). The input-output relation for the Simon certifier, see Eq. (1.11) and all related denotations, reads

$$\mathcal{W}_{\text{atm}} = \mathcal{W}_{\langle T_a^2 \rangle, \langle T_b^2 \rangle, 1} + N + \boldsymbol{\nu}^\dagger S \boldsymbol{\nu} + \boldsymbol{\mu}^\dagger F \boldsymbol{\mu}. \quad (4.15)$$

Here,  $\mathcal{W}_{\langle T_a^2 \rangle, \langle T_b^2 \rangle, 1}$  is the Simon certifier for a deterministic-loss channel with transmittances  $\langle T_a^2 \rangle$  and  $\langle T_b^2 \rangle$  [277];  $\boldsymbol{\nu} = (\langle \hat{a} \rangle, \langle \hat{a}^\dagger \rangle, \langle \hat{b} \rangle, \langle \hat{b}^\dagger \rangle)^\text{T}$ ;  $\boldsymbol{\mu} = (\langle \hat{a} \rangle \langle \hat{b} \rangle, \langle \hat{a}^\dagger \rangle \langle \hat{b} \rangle, \langle \hat{a}^\dagger \rangle \langle \hat{b}^\dagger \rangle, \langle \hat{a} \rangle \langle \hat{b}^\dagger \rangle)^\text{T}$ ;  $N$ ,  $S$ , and  $F$  are a scalar and  $4 \times 4$  matrices, respectively, which depend on the elements of the matrix  $V$ , cf. Eq. (1.12), and on the first two moments of the transmission coefficients  $T_a$  and  $T_b$ , see Ref. [XIX] for details<sup>7</sup>.

Similar to Eq. (4.14) for the squeezing certifier, we separate the contributions from the deterministic loss channel [the first term in Eq. (4.15)] from the atmospheric turbulence (the three other terms) for the Simon certifier. Unlike the case of quadrature squeezing, for which the turbulence-related term is always positive, in Eq. (4.15) only the terms  $N$  and  $\boldsymbol{\mu}^\dagger F \boldsymbol{\mu}$  are positive in the general case. An important consequence of this input-output relation is the dependence on the coherent amplitudes of the state at the receiver, i.e. on the vectors  $\boldsymbol{\nu}$  and  $\boldsymbol{\mu}$ . This is a special feature of fluctuating-loss channels, which differs from the deterministic-loss channels as well as from other Gaussian channels. One should also note that there exists a broad class of Gaussian entangled states, which always preserves Gaussian entanglement in deterministic-loss channels, i.e.  $\mathcal{W}_{\langle T_a^2 \rangle, \langle T_b^2 \rangle, 1} < 0$  if the initial state is entangled [277, 278].

<sup>7</sup> $N$ ,  $S$ , and  $F$  are related to  $\mathcal{N}$ ,  $\mathcal{S}$ , and  $\mathcal{F}$  in Ref. [XIX] as  $N = (1 - \Gamma^2)(\mathcal{N} - \mathcal{W}_{\langle T_a^2 \rangle, \langle T_b^2 \rangle, 1})$ ,  $\boldsymbol{\nu}^\dagger S \boldsymbol{\nu} = \vec{\nu}^\dagger \mathcal{S} \vec{\nu}$ ,  $\boldsymbol{\mu}^\dagger F \boldsymbol{\mu} = (1 - \Delta \Gamma^2) \mathcal{F}$ .

First, we consider the scenario of uncorrelated channels, i.e.  $\mathcal{P}(T_a, T_b) = \mathcal{P}(T_a) \mathcal{P}(T_b)$ . This is realized in the most common case of counterpropagation. In this case, the matrix  $S$  in the input-output relation (4.15) is positive definite. Hence, the best scenario for preserving the entanglement is the case of zero coherent amplitudes,  $\langle \hat{a} \rangle = \langle \hat{b} \rangle = 0$ . In this scenario an interesting effect appears if we consider the dependence on the squeezing  $\xi$  of the two-mode squeezed vacuum state  $|\text{TMSV}\rangle = (\cosh \xi)^{-1} \sum_{n=0}^{\infty} (\tanh \xi)^n |n, n\rangle$ , see Fig. 4.8. It turns out that for large values of the squeezing parameter the Gaussian entanglement vanishes.

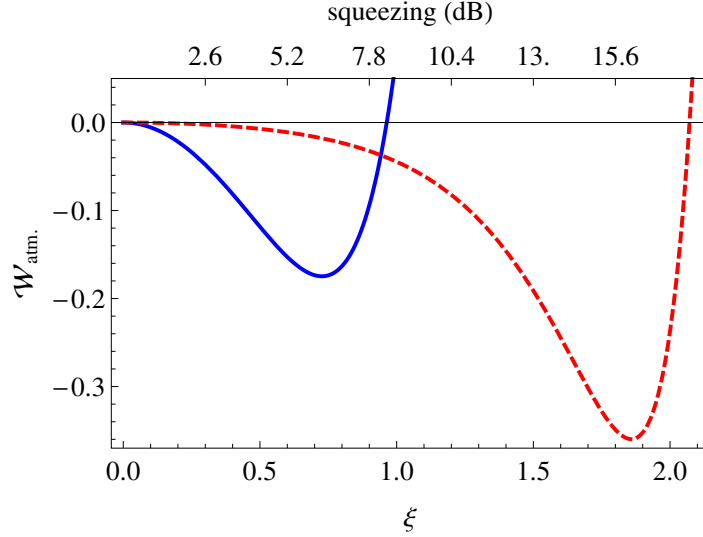


Figure 4.8: The Simon entanglement certifier  $\mathcal{W}_{\text{atm}}$  is shown for a two-mode squeezed vacuum state for two uncorrelated atmospheric channels. The solid and dashed line corresponds to the 144km-long channel on the Canary Islands and to the 1.6km long channel in Erlangen, respectively.  $\mathcal{W}_{\text{atm}}$  is scaled by  $10^6$  for the solid line. For more details see Ref. [XIX].

Second, we consider the case of completely correlated channels,  $\mathcal{P}(T_a, T_b) = \mathcal{P}(T_a) \delta(T_a - T_b)$ . In this case, the input-output relation (4.15) is reduced to

$$\mathcal{W}_{\text{atm}} = \mathcal{W}_{\langle T_a^2 \rangle, \langle T_b^2 \rangle, 1} + \nu^\dagger S \nu, \quad (4.16)$$

i.e.  $N = 0$ ,  $F = 0$ . This means that in absence of coherent displacement,  $\nu = 0$ , the entanglement dynamics corresponds to the case of deterministic-loss channels. Moreover, because the matrix  $S$  in this case is sign indefinite, there exist such directions of coherent shifting, which always preserve entanglement, see Fig. 4.8.

The scenario of correlated channels can be realized in the case of copropagation as it is considered in Ref. [90] for the Bell nonlocality test. Another way to realize such a correlation is to apply the adaptive scheme proposed in Ref. [XIX]. For this purpose we should perform the following steps: (i) measure the transmission coefficients in both channels; (ii) share this information via classical channels; (iii) attenuate the channel with the higher transmittance up to the level of channel with the lower one. Despite of the fact that in this scheme we introduce more losses in the channel, correlations of the corresponding transmittances appear to be more important for preserving the Gaussian entanglement. In Fig. 4.9, we have shown the regions of the coherent amplitudes where the entanglement is preserved for the displaced two-mode squeezed vacuum state. It is important that there exists a channel-independent part of this region, which is defined by applying the same consideration with the matrix of the DGCZ criteria, cf. Eq. (1.13).

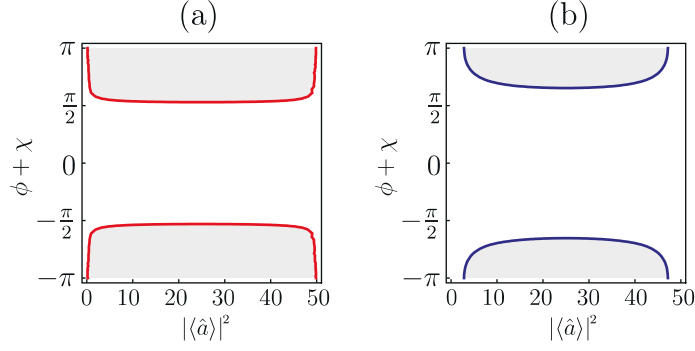


Figure 4.9: The regions (grey area) of the coherent amplitudes  $\langle \hat{a} \rangle = |\langle \hat{a} \rangle| e^{i\phi}$ ,  $\langle \hat{b} \rangle = |\langle \hat{b} \rangle| e^{i\chi}$  preserving the Gaussian entanglement for the displaced two-mode squeezed vacuum state with  $\xi = 0.5$ . We consider the case with  $|\langle \hat{a} \rangle|^2 + |\langle \hat{b} \rangle|^2 = 50$ . (a): The weak to moderate-turbulence 1.6km-long channel in Erlangen. (b): The strong-turbulence 144km-long channel on the Canary Islands. See Ref. [XIX] for more details.

#### 4.7 Higher-order nonclassical effects

In this section, I will give a brief overview on some results of Ref. [XX], where we have considered non-Gaussian entanglement and higher-order nonclassicality effects in atmospheric channels. Similar to the case of quadrature squeezing and Gaussian entanglement, we consider input-output relations for the corresponding certifiers. The first example, which was also considered in Ref. [XI], is the sub-Poissonian statistics of light. For the corresponding certifier, the Mandel Q parameter (1.6), the input-output relation reads

$$Q_{\text{out}} = \frac{\langle \eta^2 \rangle}{\langle \eta \rangle} Q_{\text{in}} + \frac{\langle \Delta \eta^2 \rangle}{\langle \eta \rangle} \langle \hat{n} \rangle_{\text{in}}. \quad (4.17)$$

This input-output relations resemble other nonclassicality tests such that the first term is similar to that for deterministic-attenuation channels and the second term is caused by the atmospheric turbulence. An important consequence of this consideration is that for intense light, for which

$$\langle \hat{n} \rangle_{\text{in}} \geq -\frac{\langle \eta^2 \rangle}{\langle \Delta \eta^2 \rangle} Q_{\text{in}}, \quad (4.18)$$

the sub-Poissonian light statistics cannot be verified anymore.

Another example is the  $k$ th-order amplitude squeezing [279], for which the certifier is given by

$$d_k = \det A_k < 0, \quad (4.19)$$

where

$$A_k = \begin{pmatrix} \langle \Delta \hat{a}^{\dagger k} \Delta \hat{a}^k \rangle & \langle (\Delta \hat{a}^k)^2 \rangle \\ \langle (\Delta \hat{a}^{\dagger k})^2 \rangle & \langle \Delta \hat{a}^{\dagger k} \Delta \hat{a}^k \rangle \end{pmatrix}. \quad (4.20)$$

The input-output relation for this certifier reads

$$d_k^{\text{out}} = \langle T^{2k} \rangle^2 d_k + \langle (\Delta T^k)^2 \rangle (\langle \hat{a}^{\dagger k} \rangle, \langle \hat{a}^k \rangle) A_k \begin{pmatrix} \langle \hat{a}^k \rangle \\ \langle \hat{a}^{\dagger k} \rangle \end{pmatrix}. \quad (4.21)$$

The first term of this relation resembles the input-output relation for a deterministic-loss channel and the second one is caused by the atmospheric turbulence.

We also consider entanglement criteria beyond the Gaussian certifier. For this purpose we consider one of the higher-order minors of the SV criteria, cf. Sec. 1.4,

$$\mathcal{W} = \det \begin{pmatrix} 1 & \langle \hat{a} \hat{b}^\dagger \rangle \\ \langle \hat{a}^\dagger \hat{b} \rangle & \langle \hat{a}^\dagger \hat{a} \hat{b}^\dagger \hat{b} \rangle \end{pmatrix} < 0. \quad (4.22)$$

This certifier has been used in Ref. [280] for the experimental verification of entanglement in the case when the Gaussian test fails. The input-output relation for this certifier is given by

$$\mathcal{W}_{\text{out}} = \langle T_a^2 T_b^2 \rangle \mathcal{W}_{\text{in}} + (\langle T_a^2 T_b^2 \rangle - \langle T_a T_b \rangle^2) |\langle \hat{a} \hat{b}^\dagger \rangle|^2. \quad (4.23)$$

The parts corresponding to deterministic losses and the atmospheric turbulence are also clearly separated for this certifier. In Ref. [XX], we are reporting on an example, which shows that non-Gaussian entanglement can be more robust in atmospheric channels compared to the Gaussian entanglement, assuming that the mean number of photons is equal in both cases.

## 4.8 Summary

In this chapter, I have reported on our results related to quantum optics in atmospheric channels. Although the atmospheric turbulence is a very complicated phenomenon, the propagation of quantum light through free-space channels can be represented by compact input-output relations. The main characteristics of such channels is the probability distribution of the transmittance (PDT). Depending on the atmospheric conditions and the beam parameters, the form of the PDT varies between the log-negative Weibull and the truncated log-normal distributions.

Furthermore, we have studied nonclassical phenomena for light at the receiver after transmission through free-space channels. Despite of disturbing effects of the atmosphere, many nonclassical and quantum effects can still be verified for such scenarios. We can also consider special procedures, which enables us to preserve the corresponding properties. The postselection assumes the direct measurement of the channel transmittance and choosing only those events with highly transparent channels. For transmitting Gaussian entanglement, one can use an adaptive scheme, which makes the transmittances of the communication channels correlated at the expense of additional losses. In the case of co-propagation, the Bell-nonlocality test has an internal postselection procedure: In this case, the events with transparent channels have a larger probability to be counted compared to the case of opaque channels.

Therefore, the proposed theory makes a significant contribution to the atmospheric quantum optics. Our findings describe experimental data very well, such as those obtained at the Max Planck Institute for the Science of Light (Erlangen). We believe that our results will be useful for the optimal design of QKD protocols in free-space channels.

## 5 Conclusions

In my cumulative habilitation thesis, I have reported of new theoretical concepts to describe the effects of noisy environment and imperfect measurements on nonclassical and quantum properties of light. Nonclassicality as well as quantumness is the main resource in quantum information and communication. We define nonclassicality as the impossibility to explain observed phenomena in the framework of classical theory. Hence, nonclassical phenomena cannot be effectively modelled by any classical system. At the same time, quantumness is the need for the system to follow boundaries restricted by the quantum theory even if these boundaries are allowed by the classical theory. We have considered important examples, which appear at three stages of communication protocols—generation, detection, and transmission of quantum states of light.

Leaky cavities are important devices, which are included in many sources of quantum light. We have proposed a noise-theory approach, which completely describes unwanted losses in such cavities also in the case when quantum-state extraction is combined with reflection of light from the cavity. The phenomenological parameters, which appear in our consideration, can be reconstructed with the proposed operational procedures. Also, these parameters are obtained from first principles in the framework of a quantum-field-theoretical approach.

Based on the proposed theory, we have analysed the quantum-state extraction from cavities. If we use leaky cavities for generating single-photon states, the nonclassicality with respect to the Wigner function is very hard to preserve with the presently available technologies. This means, that it is very hard to verify the nonclassical properties of single-photon states from such sources by using the balanced homodyne detection. At the same time, the nonclassicality with respect to the Glauber-Sudarshan  $P$  function will be preserved for any amount of losses. Hence, the measurements performed with photocounting or with unbalanced homodyne detection may have properties, which are impossible to explain by classical theories.

A consequence of our theory is the predicted effect of the loss-induced mode coupling. It turns out that only in the presence of losses through absorption and scattering, the intracavity mode can interfere with a pulse reflected from the cavity. Because such losses are unavoidable for cavities, we propose to use this effect for local quantum-state reconstruction of the intracavity mode.

Another chapter is devoted to the consideration of noise and imperfect measurement appearing in the photodetection process. Particularly, we have introduced a consistent model of multimode thermal light, which demonstrates why dark counts and stray light can be considered as additive Poissonian noise. We have proposed a numerical method, which gives a possibility to reconstruct the photon-number statistics from the measured noisy and lossy photocounting statistics. We have also shown that noise counts do not destroy the sub-Poissonian statistics of photocounts.

The impossibility to discriminate between adjacent photon numbers may result in surprising results for Bell-inequality tests. We have considered a standard scheme for testing Bell nonlocality involving a parametric down-conversion source. In this case, the measured Bell parameter may demonstrate violations beyond the quantum Tsirelson bound. This result shall not be explained as witnessing of post-quantum physics, because all calculations have been performed in framework of standard quantum theory. However, it demonstrates the importance of a correct mapping between indefinite- and finite-dimensional Hilbert spaces—the so-called squash model.

We have also found that the quantum measurements allow a clear interpretation with the methods of analytical geometry. By introducing the concept of the covariant operator-valued measure (COVM), we have proposed the method of reconstructing the mean values of observables based on measured statistics of another observable. Our theory has been

applied to the click (array and time-multiplexing) detectors, which give only a finite set of outcomes. Particularly, we have applied the developed method to the local quantum-state reconstruction with the unbalanced homodyne detection.

A theory of quantum atmospheric channels has been also considered in the thesis. We have formulated quantum-state input-output relations for such channels. The most important characteristics of the free-space channels is the probability distribution of the transmittance (PDT). We have proposed three models of the PDT, which are applicable for different atmospheric conditions. Our theoretical results are in good agreement with experimental data obtained at the Max Planck Institute for the Science of Light (Erlangen) including the case of diverse weather conditions.

We have analysed a Bell-nonlocality test using the developed techniques. For the co-propagation scenario, as it has been used in an experiment of Anton Zeilinger's group on the Canary Islands, we have found that fluctuating-loss channels may demonstrate much better violations of Bell inequalities in comparison with the deterministic-loss channels of the same transmittance. For the counterpropagation scenario, we have considered a postselection scheme, which tests the channel transmittance by intense light-pulses.

For a number of nonclassical phenomena, we have obtained the input-output relations for the corresponding tests. As a rule of thumbs, many important properties disappear by increasing the light intensity. Particularly, this is the case for quadrature squeezing.

We have studied a postselection procedure which significantly improves the quadrature squeezing. Our theoretical consideration of this fact is in good agreement with the experimental data obtained earlier at the Max Planck Institute for the Science of Light (Erlangen).

The input-output relation for the Simon test of the Gaussian entanglement have also demonstrated that in the most general scenario, the transfer of entangled states with zero coherent amplitudes are the best choice to preserve Gaussian entanglement. However, it turns out that in the case of counterpropagation, large squeezing parameters of Gaussian entangled states may destroy the entanglement at the receiver. Hence, for the corresponding experiments, large squeezing can be disadvantageous. We have proposed an adaptive scheme which enables to preserve Gaussian entanglement at the cost of additional losses. With this scheme, we are able to transfer not only entangled states with the zero coherent amplitudes but also displaced Gaussian entangled states. We believe that this finding will be useful for design of CV QKD protocols in free-space channels.

## Outlook

As an outlook for my future research, I have to note that the considered topics still have a number of open questions. From my point of view, a much better consideration should be applied to the clarification of the most fundamental relations between classical and quantum theories. Particularly, we have to understand better the relations between Bell nonlocality, contextuality and negativities of the phase-space functions. This shall provide a deeper understanding of the resources of quantum information and communication.

In the photodetection theory, there still exist some schemes which require consistent theoretical considerations. For example, the often used scheme of continuous-wave detection shall be analysed and disturbing effects, such as the detector dead time and after-pulses shall be included in the theory.

For the atmospheric channels, we still need a unified approach which enables us to better understand the changes of the PDT between log-negative Weibull and log-normal distributions. We also have to analyse time coherence in atmospheric channels, which gives us an answer on the question about the applicability of postselection procedures with high intensity light pulses. Also, a very promising idea is the use of dispersion-free light beams proposed in the group of Prof. A. Szameit for realizing high-transmittance free-space channels. This requires a generalization of our PDT theory for such beams. I believe that with such an



approach, one can design long-distance satellite-mediated channels with much better characteristics as it is used now. In my future research, I hope to contribute to these promising scientific activities.

## Bibliography

- [1] C. E. Shannon, Communication Theory of Secrecy Systems, *Bell Syst. Technol. J.* **28**, 656 (1949).
- [2] C. E. Shannon and W. Weaver, *The mathematical theory of communication*, (Univ. Illinois Press, Urbana Ill. 1949)
- [3] W. Vogel and D.-G. Welsch, *Quantum Optics*, (Wiley–VCH, Berlin, 2006).
- [4] W.P. Schleich, *Quantum optics in phase space*, (Wiley–WCH, Berlin, 2001).
- [5] J. von Neumann, Wahrscheinlichkeitstheoretischer Aufbau der Quantenmechanik, *Göttinger Nachrichten* **1**, 245 (1927).
- [6] L. Landau, Das Dämpfungsproblem in der Wellenmechanik, *Z. Phys.* **45**, 430 (1927).
- [7] E. Joos and H.D. Zeh, The emergence of classical properties through interaction with the environment, *Z. Physik B* **59**, 223 (1985).
- [8] C. W. Helstrom, *Quantum Detection and Estimation Theory*, (Academic Press, Inc.1976)
- [9] A. S. Holevo, *Statistical structure of quantum theory* (Springer, Berlin-Heidelberg, 2001).
- [10] A. Menezes, P. van Oorschot, and S. Vanstone, *Handbook of Applied Cryptography*, (CRC Press, Inc., 1997).
- [11] R. L. Rivest, A. Shamir, and L. Adleman, A method for obtaining digital signatures and public-key cryptosystems, *Communications of the ACM* **21**, 120 (1978).
- [12] M. A. Nielsen and I. L. Chuang, *Quantum Computation and Quantum Information*, (Cambridge University Press, Cambridge, 2010).
- [13] P. W. Shor, Algorithms for quantum computation: discrete logarithms and factoring, 2013 IEEE 54th Annual Symposium on Foundations of Computer Science **00**, 124 (1994).
- [14] P. W. Shor, Polynomial-Time Algorithms for Prime Factorization and Discrete Logarithms on a Quantum Computer, *S.I.A.M. Journal of Computing*, **26**, 1484 (1997).
- [15] N. Gisin, G. Ribordy, W. Tittel, and H. Zbinden, Quantum cryptography, *Rev. Mod. Phys.* **74**, 145195 (2002).
- [16] N. Gisin and R. Thew, Quantum Communication, *Nature Photon.* **1**, 165 (2007).
- [17] C. H. Bennett and G. Brassard, Quantum cryptography: Public key distribution and coin tossing, in *Proc. IEEE Int. Conf. on Computers, Systems and Signal Processing*, (IEEE, New York, 1984).
- [18] C. H. Bennett, Quantum cryptography using any two nonorthogonal states, *Phys. Rev. Lett* **68**, 3121 (1992).
- [19] D. Bruß, Optimal Eavesdropping in Quantum Cryptography with Six States, *Phys. Rev. Lett* **81**, 3018 (1998).
- [20] V. Scarani, A. Acin, G. Ribordy, and N. Gisin, Quantum Cryptography Protocols Robust against Photon Number Splitting Attacks for Weak Laser Pulse Implementations, *Phys. Rev. Lett.* **92**, 057901 (2004).

- [21] W.-Y. Hwang, Quantum Key Distribution with High Loss: Toward Global Secure Communication, *Phys. Rev. Lett.* **91**, 057901 (2003).
- [22] H.-K. Lo, H.F. Chau, and M. Ardehali, Efficient Quantum Key Distribution Scheme And Proof of Its Unconditional Security, *Journal of Cryptology* **18**, 133 (2005).
- [23] A. Ekert, Quantum cryptography based on Bell's theorem, *Phys. Rev. Lett.* **67**, 661 (1991).
- [24] A. Acín, N. Gisin, and L. Masanes, From Bell's Theorem to Secure Quantum Key Distribution, *Phys. Rev. Lett.* **97**, 120405 (2006).
- [25] A. Acín, N. Brunner, N. Gisin, S. Massar, S. Pironio, and V. Scarani, Device-Independent Security of Quantum Cryptography against Collective Attacks, *Phys. Rev. Lett.* **98**, 230501 (2007).
- [26] C.H. Bennett, G. Brassard, N. D. Mermin, *Phys. Rev. Lett.* **68**, 557 (1992).
- [27] A. C. Funk and M. G. Raymer, Quantum key distribution using nonclassical photon-number correlations in macroscopic light pulses, *Phys. Rev. A* **65**, 042307 (2002).
- [28] M. Hillery, Quantum cryptography with squeezed states, *Phys. Rev. A* **61**, 022309 (1999).
- [29] T. C. Ralph, Continuous variable quantum cryptography, *Phys. Rev. A* **61**, 010303 (2000).
- [30] T. C. Ralph, Security of continuous-variable quantum cryptography, *Phys. Rev. A* **62**, 062306 (2000).
- [31] S. F. Pereira, Z. Y. Ou, and H. J. Kimble, Quantum communication with correlated nonclassical states, *Phys. Rev. A* **62**, 042311 (2000).
- [32] M. D. Reid, Quantum cryptography with a predetermined key, using continuous-variable Einstein-Podolsky-Rosen correlations, *Phys. Rev. A* **62**, 062308 (2000).
- [33] N. J. Cerf, M. Levy and G. Van Assche, Quantum distribution of Gaussian keys using squeezed states, *Phys. Rev. A* **63**, 052311 (2001).
- [34] D. Gottesman and J. Preskill, Secure quantum key distribution using squeezed states, *Phys. Rev. A* **63**, 022309 (2001).
- [35] F. Grosshans and P. Grangier, Continuous Variable Quantum Cryptography Using Coherent States, *Phys. Rev. Lett.* **88**, 057902 (2002).
- [36] F. Grosshans, G. V. Assche, R. M. Wenger, R. Brouri, N. J. Cerf, and P. Grangier, Quantum key distribution using gaussian-modulated coherent states, *Nature* **421**, 238 (2003).
- [37] Ch. Silberhorn, N. Korolkova, and G. Leuchs, Quantum Key Distribution with Bright Entangled Beams, *Phys. Rev. Lett.* **88**, 167902 (2002).
- [38] L.S. Madsen, V.C. Usenko, M. Lassen, R. Filip, and U.L. Andersen, Continuous variable quantum key distribution with two-mode squeezed states, *Nat. Commun.* **3**, 1083 (2012).
- [39] S. L. Braunstein and P. van Loock, Quantum information with continuous variables, *Rev. Mod. Phys.* **77**, 513 (2005).

- [40] C. Zachos, D. Fairlie, and T. Curtright, *Quantum Mechanics in Phase Space* (World Scientific, Singapore, 2005).
- [41] Yu. M. Shirokov, Quantum and classical mechanics in the phase-space representation, *Sov. J. Part. Nucl.* **10**, 1 (1979).
- [42] J.E. Moyal, Quantum mechanics as a statistical theory, *Proc. Cambr. Phil. Soc.* **45**, 99 (1949).
- [43] D.-G. Welsch, W. Vogel, T. Opatrný, Homodyne Detection and Quantum State Reconstruction, *Progr. Opt.* **39**, 63 (1999).
- [44] J. H. Shapiro, H. P. Yuen, and J. A. Machado Mata, Optical communication with two-photon coherent states—Part II: Photoemissive detection and structured receiver performance, *IEEE Trans. Inf. Theory* **25**, 179 (1979).
- [45] H. Yuen and J. Shapiro, Optical communication with two-photon coherent states—Part III: Quantum measurements realizable with photoemissive detectors, *IEEE Trans. Inf. Theory* **26**, 78 (1980).
- [46] H. P. Yuen and V. W. S. Chan, Noise in homodyne and heterodyne detection, *Opt. Lett.* **8**, 177 (1983).
- [47] G. L. Abbas, V. W. S. Chan, and T. K. Yee, Local-oscillator excess-noise suppression for homodyne and heterodyne detection, *Opt. Lett.* **8**, 419 (1983).
- [48] L. Mandel, Squeezed States and Sub-Poissonian Photon Statistics, *Phys. Rev. Lett.* **49**, 136 (1982).
- [49] B. L. Schumaker, Noise in homodyne detection, *Opt. Lett.* **9**, 189 (1984).
- [50] B. Yurke, Squeezed-coherent-state generation via four-wave mixers and detection via homodyne detectors, *Phys. Rev. A* **32**, 300 (1985).
- [51] K. Vogel and H. Risken, Determination of quasiprobability distributions in terms of probability distributions for the rotated quadrature phase, *Phys. Rev. A* **40**, 2847 (1989).
- [52] D.T. Smithey, M. Beck, M.G. Raymer, A. Faridani, Measurement of the Wigner distribution and the density matrix of a light mode using optical homodyne tomography: Application to squeezed states and the vacuum, *Phys. Rev. Lett.* **70**, 1244 (1993).
- [53] A. Zavatta, V. Parigi, and M. Bellini, Experimental nonclassicality of single-photon-added thermal light states, *Phys. Rev. A* **75**, 052106 (2007).
- [54] E. P. Wigner, On the Quantum Correction For Thermodynamic Equilibrium, *Phys. Rev.* **40**, 749 (1932).
- [55] Yu. A. Brychkov and A. P. Prudnikov, *Integral Transforms of Generalized Functions*, (CRC Press, 1989).
- [56] L. Mandel, E. Wolf, *Optical coherence and quantum optics*, (Cambridge University Press, 1995).
- [57] P. L. Kelley and W. H. Kleiner, Theory of Electromagnetic Field Measurement and Photoelectron Counting, *Phys. Rev.* **136**, A316 (1964).
- [58] R. J. Glauber, Coherent and incoherent states of the radiation field, *Phys. Rev. A* **131**, 2766 (1963).

- [59] E. C. G. Sudarshan, Equivalence of Semiclassical and Quantum Mechanical Descriptions of Statistical Light Beams, *Phys. Rev. Lett.* **10**, 277 (1963).
- [60] J. Klauder and E.C.G. Sudarshan, *Fundamentals of Quantum Optics*, (Dover Publications Inc., 2006).
- [61] U. M. Titulaer and R. J. Glauber, Correlation Functions for Coherent Fields, *Phys. Rev.* **140**, B676 (1965).
- [62] W. Vogel, Nonclassical states: An observable criterion, *Phys. Rev. Lett.* **84**, 1849 (2000).
- [63] Th. Richter and W. Vogel, Nonclassicality of quantum states: a hierarchy of observable conditions, *Phys. Rev. Lett.* **89**, 283601 (2002).
- [64] E. Shchukin, Th. Richter, and W. Vogel, Nonclassicality criteria in terms of moments, *Phys. Rev. A* **71**, 011802(R) (2005).
- [65] T. Kiesel and W. Vogel, Nonclassicality filters and quasi-probabilities, *Phys. Rev. A* **82**, 032107 (2010).
- [66] F. Shahandeh, A. P. Lund, and T. C. Ralph, Quantum Correlations in Nonlocal Boson Sampling, *Phys. Rev. Lett.* **119**, 120502 (2017).
- [67] S. Scheel, Permanents in linear optical networks, *Acta Physica Slovaca.* **58**, 675 (2008).
- [68] S. Aaronson and A. Arkhipov, The Computational Complexity of Linear Optics, *Theory of Computing.* **9**, 143 (2013).
- [69] L. Mandel, Sub-Poissonian photon statistics in resonance fluorescence, *Opt. Lett.* **4**, 205 (1979).
- [70] N. G. Walker, Quantum theory of multiport optical homodyning, *J. Mod. Opt.* **34**, 15 (1987).
- [71] K. Husimi, Some Formal Properties of the Density Matrix, *Proc. Phys. Math. Soc. Japan* **22**, 264 (1970).
- [72] Y. Kano, A New Phase-Space Distribution Function in the Statistical Theory of the Electromagnetic Field, *J. Math. Phys.* **6**, 1913 (1965).
- [73] G. Adesso, S. Ragy, and A. R. Lee, Continuous Variable Quantum Information: Gaussian States and Beyond, *Open Syst. Inf. Dyn.* **21**, 1440001 (2014).
- [74] L.-A. Wu, H. J. Kimble, J. L. Hall, and H. Wu, Generation of Squeezed States by Parametric Down Conversion, *Phys. Rev. Lett.* **57**, 2520 (1986).
- [75] L.-A. Wu, M. Xiao, and H. J. Kimble Squeezed states of light from an optical parametric oscillator, *J. Opt. Soc. Am. B* **4**, 1465 (1987).
- [76] H. Vahlbruch, M. Mehmet, K. Danzmann, and R. Schnabel, Detection of 15 dB Squeezed States of Light and their Application for the Absolute Calibration of Photoelectric Quantum Efficiency, *Phys. Rev. Lett.* **117**, 110801 (2016).
- [77] D. Stoler, Equivalence Classes of Minimum Uncertainty Packets, *Phys. Rev. D* **1**, 3217 (1970).
- [78] D. Stoler, Equivalence Classes of Minimum-Uncertainty Packets. II, *Phys. Rev. D* **4**, 1925 (1971).

- [79] H.P. Yuen, Two-photon coherent states of the radiation field, *Phys. Rev. A* **13**, 2226 (1976).
- [80] W. Heisenberg, Über den anschaulichen Inhalt der quantentheoretischen Kinematik und Mechanik, *Z. Physik*, **43**, 172 (1927).
- [81] N. Brunner, D. Cavalcanti, S. Pironio, V. Scarani, and S. Wehner, Bell Nonlocality, *Rev. Mod. Phys.* **86**, 419 (2014).
- [82] J. S. Bell, On the Einstein Podolsky Rosen paradox, *Physics* **1**, 195 (1964).
- [83] J. F. Clauser, M. A. Horn, A. Shimony, and R. A. Holt, Proposed Experiment to Test Local Hidden Variable Theories, *Phys. Rev. Lett.* **23**, 880 (1969).
- [84] A. Fine, Hidden Variables, Joint Probability, and the Bell Inequality, *Phys. Rev. Lett.* **48**, 291 (1982).
- [85] B. S. Cirel'son, Quantum Generalizations of Bell's Inequalities, *Lett. Math. Phys.* **4**, 93 (1980).
- [86] S. Popescu and D. Rohrlich, Quantum Nonlocality as an Axiom, *Found. Phys.* **24**, 379 (1994).
- [87] S. J. Freedman and J. F. Clauser, Experimental Test of Local Hidden-Variable Theories, *Phys. Rev. Lett.* **28**, 938 (1972).
- [88] A. Aspect, J. Dalibard, and G. Roger, Experimental Test of Bell's Inequalities Using Time-Varying Analyzers, *Phys. Rev. Lett.* **49**, 1804 (1982).
- [89] R. Ursin *et al.*, Entanglement-Based Quantum Communication over 144 km, *Nat. Phys.* **3**, 481 (2007).
- [90] A. Fedrizzi, R. Ursin, T. Herbst, M. Nespoli, R. Prevedel, T. Scheidl, F. Tiefenbacher, T. Jennewein, and A. Zeilinger, High-Fidelity Transmission of Entanglement over a High-Loss Free-Space Channel, *Nat. Phys.* **5**, 389 (2009).
- [91] J. Yin *et al.*, Satellite-based entanglement distribution over 1200 kilometers, *Science* **356**, 1140 (2017).
- [92] R. Horodecki, P. Horodecki, M. Horodecki, and K. Horodecki, Quantum entanglement, *Rev. Mod. Phys.* **81**, 865 (2009).
- [93] A. Einstein, B. Podolsky, N. Rosen, Can Quantum-Mechanical Description of Physical Reality Be Considered Complete? *Phys. Rev.* **47**, 777 (1935).
- [94] R. F. Werner, Quantum states with Einstein-Podolsky-Rosen correlations admitting a hidden-variable model, *Phys. Rev. A* **40**, 4277 (1989).
- [95] J. Sperling and W. Vogel, Necessary and sufficient conditions for bipartite entanglement, *Phys. Rev. A* **79**, 022318 (2009).
- [96] J. Sperling and W. Vogel, Representation of entanglement by negative quasiprobabilities, *Phys. Rev. A* **79**, 042337 (2009).
- [97] A. Peres, Separability Criterion for Density Matrices, *Phys. Rev. Lett.* **77**, 1413 (1996).
- [98] M. Horodecki, P. Horodecki, and R. Horodecki, Separability of mixed states: necessary and sufficient conditions, *Phys. Lett. A* **223**, 1 (1996).

- [99] M. Horodecki, P. Horodecki, and R. Horodecki, Mixed-State Entanglement and Distillation: Is there a Bound Entanglement in Nature? *Phys. Rev. Lett.* **80**, 5239 (1998).
- [100] E. Shchukin and W. Vogel, Inseparability Criteria for Continuous Bipartite Quantum States, *Phys. Rev. Lett.* **95**, 230502 (2005).
- [101] R. Simon, Peres-Horodecki Separability Criterion for Continuous Variable Systems, *Phys. Rev. Lett.* **84**, 2726 (2000).
- [102] L.-M. Duan, G. Giedke, J. I. Cirac, and P. Zoller, Inseparability Criterion for Continuous Variable Systems, *Phys. Rev. Lett.* **84**, 2722 (2000).
- [103] S. L. Braunstein and H. J. Kimble, Teleportation of Continuous Quantum Variables, *Phys. Rev. Lett.* **80**, 869 (1998).
- [104] P. van Loock and S. L. Braunstein, Unconditional teleportation of continuous-variable entanglement, *Phys. Rev. A* **61**, 010302(R) (1999).
- [105] S. Lloyd and S. L. Braunstein, Quantum Computation over Continuous Variables, *Phys. Rev. Lett.* **82**, 1784 (1999).
- [106] F. Soto and P. Claverie, When is the Wigner function of multidimensional systems nonnegative? *J. Math. Phys.* **24**, 97 (1983).
- [107] S. D. Bartlett, B. C. Sanders, S. L. Braunstein, and K. Nemoto, Efficient Classical Simulation of Continuous Variable Quantum Information Processes, *Phys. Rev. Lett.* **88**, 097904 (2002).
- [108] A. Mari and J. Eisert, Positive Wigner Functions Render Classical Simulation of Quantum Computation Efficient, *Phys. Rev. Lett.* **109**, 230503 (2012).
- [109] U. Chabaud, T. Douce, D. Markham, P. van Loock, E. Kashefi, and G. Ferrini, Continuous-variable sampling from photon-added or photon-subtracted squeezed states, *Phys. Rev. A* **96**, 062307 (2017).
- [110] N. C. Menicucci, P. van Loock, M. Gu, Ch. Weedbrook, T. C. Ralph, and M. A. Nielsen, Universal Quantum Computation with Continuous-Variable Cluster States, *Phys. Rev. Lett.* **97**, 110501 (2006).
- [111] K. E. Cahill and R. J. Glauber, Ordered Expansions in Boson Amplitude Operators, *Phys. Rev.* **177**, 1857 (1969).
- [112] K. E. Cahill and R. J. Glauber, Density Operators and Quasiprobability Distributions, *Phys. Rev.* **177**, 1882 (1969).
- [113] S. Wallentowitz and W. Vogel, Unbalanced homodyning for quantum state measurements, *Phys. Rev. A* **53**, 4528, (1996).
- [114] S. Mancini, P. Tombesi, and V. I. Man'ko, Density matrix from photon number tomography, *Europhys. Lett.* **37**, 79 (1997).
- [115] K. Banaszek, C. Radzewicz, K. Wódkiewicz, and J. S. Krasinski, Direct measurement of the Wigner function by photon counting, *Phys. Rev. A* **60**, 674 (1999).
- [116] G. Harder, Ch. Silberhorn, J. Rehacek, Z. Hradil, L. Motka, B. Stoklasa, and L.L. Sánchez-Soto, Local Sampling of the Wigner Function at Telecom Wavelength with Loss-Tolerant Detection of Photon Statistics, *Phys. Rev. Lett.* **116**, 133601 (2016).
- [117] A. E. Siegman, *Lasers*, (University Science Book, Sausalito, CA, 1986).

- [118] D. F. Walls and G.J. Milburn, *Quantum Optics*, (Springer-Verlag, Berlin, 2008).
- [119] H. Walther, B. T. H. Varcoe, B.-G. Englert, and T. Becker, Cavity quantum electrodynamics, *Rep. Prog. Phys.* **69** 1325 (2006).
- [120] R. Miller, T. E. Northup, K. M. Birnbaum, A. Boca, A. D. Boozer, and H. J. Kimble, Trapped atoms in cavity QED: coupling quantized light and matter, *J. Phys. B: At. Mol. Opt. Phys.* **38**, S551 (2005).
- [121] S. Haroche, Nobel Lecture: Controlling photons in a box and exploring the quantum to classical boundary, *Rev. Mod. Phys.* **85**, 1083 (2013).
- [122] M. Brune, S. Haroche, J. M. Raimond, L. Davidovich, and N. Zagury, Manipulation of photons in a cavity by dispersive atom-field coupling: Quantum-nondemolition measurements and generation of Schrödinger cat states, *Phys. Rev. A* **45**, 5193 (1992).
- [123] C. M. Savage, S. L. Braunstein, and D. F. Walls, Macroscopic quantum superpositions by means of single-atom dispersion, *Opt. Lett.* **15**, 628 (1990).
- [124] M. Brune, E. Hagley, J. Dreyer, X. Maître, A. Maali, C. Wunderlich, J. M. Raimond, and S. Haroche, Observing the Progressive Decoherence of the Meter in a Quantum Measurement, *Phys. Rev. Lett.* **77**, 4887 (1996).
- [125] A. Auffeves, P. Maioli, T. Meunier, S. Gleyzes, G. Nogues, M. Brune, J. M. Raimond, and S. Haroche, Entanglement of a Mesoscopic Field with an Atom Induced by Photon Graininess in a Cavity, *Phys. Rev. Lett.* **91**, 230405 (2003).
- [126] T. Meunier, S. Gleyzes, P. Maioli, A. Auffeves, G. Nogues, M. Brune, J. M. Raimond, and S. Haroche, Rabi Oscillations Revival Induced by Time Reversal: A Test of Mesoscopic Quantum Coherence, *Phys. Rev. Lett.* **94**, 010401 (2005).
- [127] S. Deléglise, I. Dotsenko, C. Sayrin, J. Bernu, M. Brune, J.-M. Raimond, and S. Haroche, Reconstruction of non-classical cavity field states with snapshots of their decoherence, *Nature* **455**, 510 (2008).
- [128] S. Haroche and J.-M. Raimond, *Exploring the Quantum: Atoms, Cavities and Photons*, (Oxford University Press, Oxford, 2006).
- [129] V. B. Braginsky, Y. I. Vorontsov, and F. Ya. Khalili, Quantum singularities of a ponderomotive meter of electromagnetic energy, *Sov. Phys. JETP* **46**, 705 (1977).
- [130] V. B. Braginsky and F. Ya. Khalili, Optico-magnetic effects in nondestructive quantum counting, *Sov. Phys. JETP* **51**, 859 (1980).
- [131] V. B. Braginsky, Yu. I. Vorontsov, K. S. Thorne, Quantum Nondemolition Measurements, *Science* **209**, 547 (1980).
- [132] M. Brune, S. Haroche, V. Lefevre, J. M. Raimond, and N. Zagury, Quantum non-demolition measurement of small photon numbers by Rydberg-atom phase-sensitive detection, *Phys. Rev. Lett.* **65**, 976 (1990).
- [133] S. Gleyzes, S. Kuhr, Ch. Guerlin, J. Bernu, S. Deléglise, U. B. Hoff, M. Brune, J.-M. Raimond, and S. Haroche, Quantum jumps of light recording the birth and death of a photon in a cavity, *Nature* **446**, 297 (2007).
- [134] Ch. Guerlin, J. Bernu, S. Deléglise, C. Sayrin, S. Gleyzes, S. Kuhr, M. Brune, J.-M. Raimond, and S. Haroche, Progressive field-state collapse and quantum non-demolition photon counting, *Nature* **448**, 889 (2007).



- [135] M. Brune, J. Bernu, C. Guerlin, S. Delglise, C. Sayrin, S. Gleyzes, S. Kuhr, I. Dotsenko, J. M. Raimond, and S. Haroche, Process Tomography of Field Damping and Measurement of Fock State Lifetimes by Quantum Nondemolition Photon Counting in a Cavity, *Phys. Rev. Lett.* **101**, 240402 (2008).
- [136] J. Krause, M. O. Scully, and H. Walther, State reduction and  $|n\rangle$ -state preparation in a high-Q micromaser, *Phys. Rev. A* **36**, 4547(R) (1987).
- [137] B. T. H. Varcoe, S. Brattke, M. Weidinger, and H. Walther, Preparing pure photon number states of the radiation field, *Nature* **403**, 743 (2000).
- [138] S. Brattke, B. T. H. Varcoe, and H. Walther, Generation of Photon Number States on Demand via Cavity Quantum Electrodynamics, *Phys. Rev. Lett.* **86**, 3534 (2001).
- [139] J. McKeever, A. Boca, A. D. Boozer, R. Miller, J. R. Buck, A. Kuzmich, H. J. Kimble, Deterministic Generation of Single Photons from One Atom Trapped in a Cavity, *Science* **303** 1992 (2004).
- [140] C. K. Law and J. H. Eberly, Arbitrary Control of a Quantum Electromagnetic Field, *Phys. Rev. Lett.* **76**, 1055 (1996).
- [141] A. S. Parkins, P. Marte, P. Zoller, O. Carnal, and H. J. Kimble, Quantum-state mapping between multilevel atoms and cavity light fields, *Phys. Rev. A* **51**, 1578 (1995).
- [142] W. Lange and H. J. Kimble, Dynamic generation of maximally entangled photon multiplets by adiabatic passage, *Phys. Rev. A* **61**, 063817 (2000).
- [143] C. Di Fidio, S. Maniscalco, W. Vogel, and A. Messina, Cavity QED with a trapped ion in a leaky cavity, *Phys. Rev. A* **65**, 033825 (2002).
- [144] C. Di Fidio and W. Vogel, W-type entanglement of distant atoms: conditional preparation, *J. Opt. B: Quantum Semiclass. Opt.* **5** 105 (2003).
- [145] J. I. Cirac, P. Zoller, H. J. Kimble, and H. Mabuchi, Quantum State Transfer and Entanglement Distribution among Distant Nodes in a Quantum Network, *Phys. Rev. Lett.* **78**, 3221 (1997).
- [146] P. J. Bardroff, E. Mayr, and W. P. Schleich, Quantum state endoscopy: Measurement of the quantum state in a cavity, *Phys. Rev. A* **51**, 4963 (1995).
- [147] M. F. Santos, L. G. Lutterbach, S. M. Dutra, N. Zagury, and L. Davidovich, Reconstruction of the state of the radiation field in a cavity through measurements of the outgoing field, *Phys. Rev. A* **63**, 033813 (2001).
- [148] M. J. Collet and C. M. Gardiner, Squeezing of intracavity and traveling-wave light fields produced in parametric amplification, *Phys. Rev. A* **30**, 1386 (1984).
- [149] C. W. Gardiner and M. J. Collet, Input and output in damped quantum systems: Quantum stochastic differential equations and the master equation, *Phys. Rev. A* **31**, 3761 (1985).
- [150] C. Gardiner and P. Zoller, *Quantum Noise: A Handbook of Markovian and Non-Markovian Quantum Stochastic Methods with Applications to Quantum Optics*, (Springer-Verlag, Berlin, 2004).
- [151] C. Viviescas and G. Hackenbroich, Field quantization for open optical cavities, *Phys. Rev. A* **67**, 013805 (2003).

- [152] C. Viviescas and G. Hackenbroich, Quantum theory of multimode fields: applications to optical resonators, *J. Opt. B: Quantum Semiclass. Opt.* **6**, 211 (2004).
- [153] H. Feshbach, A unified theory of nuclear reactions. II, *Ann. Phys. N.Y.* **19**, 287 (1962).
- [154] L. Knöll, W. Vogel, and D.-G. Welsch, Resonators in quantum optics: A first-principles approach, *Phys. Rev. A* **43**, 543 (1991).
- [155] R. W. F. van der Plank and L. G. Sutorp, Generalization of damping theory for cavities with mirrors of finite transmittivity, *Phys. Rev. A* **53**, 1791 (1996).
- [156] S. M. Dutra and G. Nienhuis, Quantized mode of a leaky cavity, *Phys. Rev. A* **62**, 063805 (2000).
- [157] S. Kuhra, S. Gleyzes, C. Guerlin, J. Bernu, U. B. Hoff, S. Deléglise, S. Osnaghi, M. Brune, and J.-M. Raimond, Ultrahigh finesse Fabry-Pérot superconducting resonator, *Appl. Phys. Lett.* **90**, 164101 (2007).
- [158] C. J. Hood, H. J. Kimble, and J. Ye, Characterization of high-finesse mirrors: Loss, phase shifts, and mode structure in an optical cavity, *Phys. Rev. A* **64**, 033804 (2001).
- [159] M. Pelton, C. Santory, J. Vučković, B. Zhang, G. S. Solomon, J. Plant, and Y. Yamamoto, Efficient Source of Single Photons: A Single Quantum Dot in a Micropost Microcavity, *Phys. Rev. Lett.* **89**, 233602 (2002).
- [160] G. Rempe, R. J. Thompson, and H. Kimble, Measurement of ultralow losses in an optical interferometer, *Opt. Lett.* **17**, 363 (1992).
- [161] Z. Kis, T. Kiss, J. Janszky, P. Adam, S. Wallentowitz, and W. Vogel, Local sampling of phase-space distributions by cascaded optical homodyning, *Phys. Rev. A* **59**, R39 (1999).
- [162] M. Munroe, D. Boggavarapu, M. E. Anderson, and M. G. Raymer, Photon-number statistics from the phase-averaged quadrature-field distribution: Theory and ultrafast measurement, *Phys. Rev. A* **52**, R924 (1995).
- [163] Th. Richter, Direct sampling of a smoothed Wigner function from quadrature distributions, *J. Opt. B* **1**, 650 (1999).
- [164] M. J. Thorpe, R. J. Jones, K.D. Moll, J. Ye, and R. Lalezari, Precise measurements of optical cavity dispersion and mirror coating properties via femtosecond combs, *Opt. Express* **13**, 882 (2005).
- [165] E. E. Mikhailov, K. Goda, and N. Mavalvala, Noninvasive measurements of cavity parameters by use of squeezed vacuum, *Phys. Rev. A* **74**, 033817 (2006).
- [166] U. Leonhardt and H. Paul, High-Accuracy Optical Homodyne Detection with Low-Efficiency Detectors: "Preamplification" from Antisqueezing, *Phys. Rev. Lett.* **72**, 4086 (1994).
- [167] U. Leonhardt and H. Paul, Measuring the quantum state of light, *Progr. Quantum Electron.* **19**, 89 (1995).
- [168] T. Kiss, U. Herzog, and U. Leonhardt, Compensation of losses in photodetection and in quantum-state measurements, *Phys. Rev. A* **52**, 2433 (1995).
- [169] U. Herzog, Loss-error compensation in quantum-state measurements and the solution of the time-reversed damping equation, *Phys. Rev. A* **53**, 1245 (1996).

- [170] U. H. Yurtsever, P. Kok, G. M. Hockney, C. Adami, S. L. Braunstein, J. P. Dowling, Towards photostatistics from photon-number discriminating detectors, *J. Mod. Opt.* **51**, 1517 (2004).
- [171] A. N. Tikhonov and V. Y. Arsenin, *Solutions of ill-posed problems*, (W. H. Winston, New York, 1977).
- [172] S. Karp, E. L. O'Neill, and R. M. Gagliardi, Communication theory for the free-space optical channel, *Proc. IEEE* **58**, 1611 (1970).
- [173] W. K. Pratt, *Laser Communication Systems*, (Wiley and Sons, NY, 1969).
- [174] P. P. Rohde and T. C. Ralph, Modelling photo-detectors in quantum optics, *J. Mod. Opt.* **53**, 1589 (2006).
- [175] M. G. A. Paris, A robust verification of the quantum nature of light, *Phys. Lett. A* **289**, 167 (2001).
- [176] N. J. Beaudry, T. Moroder, and N. Lütkenhaus, Squashing Models for Optical Measurements in Quantum Communication, *Phys. Rev. Lett.* **101**, 093601 (2008).
- [177] T. Moroder, O. Gühne, N. Beaudry, M. Piani, and N. Lütkenhaus, Entanglement verification with realistic measurement devices via squashing operations, *Phys. Rev. A* **81**, 052342 (2010).
- [178] C.-H. Fred Fung, H. F. Chau, and H. K. Lo, Universal squash model for optical communications using linear optics and threshold detectors, *Phys. Rev. A* **84**, 020303(R) (2011).
- [179] X. Ma, Chi-Hang Fred Fung, and H. K. Lo, Quantum key distribution with entangled photon sources, *Phys. Rev. A* **76**, 012307 (2007).
- [180] P. Kok and S. L. Braunstein, Postselected versus nonpostselected quantum teleportation using parametric down-conversion, *Phys. Rev. A* **61**, 042304 (2000).
- [181] D. Achilles, C. Silberhorn, C. Śliwa, K. Banaszek, and I. A. Walmsley, Fiber-assisted detection with photon number resolution, *Opt. Lett.* **28**, 2387 (2003).
- [182] M. J. Fitch, B. C. Jacobs, T. B. Pittman, and J. D. Franson, Photon-number resolution using time-multiplexed single-photon detectors, *Phys. Rev. A* **68**, 043814 (2003).
- [183] J. Řeháček, Z. Hradil, O. Haderka, J. Peřina, Jr., and M. Hamar, Multiple-photon resolving fiber-loop detector, *Phys. Rev. A* **67**, 061801(R) (2003).
- [184] H. Paul, P. Törmä, T. Kiss, and I. Jex, Photon Chopping: New Way to Measure the Quantum State of Light, *Phys. Rev. Lett.* **76**, 2464 (1996).
- [185] S. A. Castelletto, I. P. Degiovanni, V. Schettini, and A. L. Migdall, Reduced deadtime and higher rate photon-counting detection using a multiplexed detector array, *J. Mod. Opt.* **54**, 337 (2007).
- [186] V. Schettini, S. V. Polyakov, I. P. Degiovanni, G. Brida, S. Castelletto, and A. L. Migdall, Implementing a Multiplexed System of Detectors for Higher Photon Counting Rates, *IEEE J. Sel. Top. Quantum Electron.* **13**, 978 (2007).
- [187] J.-L. Blanchet, F. Devaux, L. Furfaro, and E. Lantz, Measurement of Sub-Shot-Noise Correlations of Spatial Fluctuations in the Photon-Counting Regime, *Phys. Rev. Lett.* **101**, 233604 (2008).

- [188] C. Silberhorn, Detecting quantum light, *Contemp. Phys.* **48**, 143 (2007).
- [189] J. Sperling, W. Vogel, and G. S. Agarwal, True photocounting statistics of multiple on-off detectors, *Phys. Rev. A* **85**, 023820 (2012).
- [190] J. Sperling, W. Vogel, and G. S. Agarwal, Sub-Binomial Light, *Phys. Rev. Lett.* **109**, 093601 (2012).
- [191] J. Sperling, W. Vogel, and G. S. Agarwal, Correlation measurements with on-off detectors, *Phys. Rev. A* **88**, 043821 (2013).
- [192] J. Sperling, M. Bohmann, W. Vogel, G. Harder, B. Brecht, V. Ansari, and C. Silberhorn, Uncovering Quantum Correlations with Time-Multiplexed Click Detection, *Phys. Rev. Lett.* **115**, 023601 (2015).
- [193] J. Sperling, T.J. Bartley, G. Donati, M. Barbieri, X.-M. Jin, A. Datta, W. Vogel, and I.A. Walmsley, Quantum Correlations from the Conditional Statistics of Incomplete Data, *Phys. Rev. Lett.* **117**, 083601 (2016).
- [194] A. Luis, J. Sperling, and W. Vogel, Nonclassicality Phase-Space Functions: More Insight with Fewer Detectors, *Phys. Rev. Lett.* **114**, 103602 (2015).
- [195] T. Lipfert, J. Sperling, and W. Vogel, Homodyne detection with on-off detector systems, *Phys. Rev. A* **92**, 053835 (2015).
- [196] M. Bohmann, J. Tiedau, T. Bartley, J. Sperling, C. Silberhorn, and W. Vogel, Incomplete Detection of Nonclassical Phase-Space Distributions, *arXiv:1711.10962*.
- [197] G. Harder, C. Silberhorn, J. Rehacek, Z. Hradil, L. Motka, B. Stoklasa, and L. L. Sánchez-Soto, Time-multiplexed measurements of nonclassical light at telecom wavelengths, *Phys. Rev. A* **90**, 042105 (2014).
- [198] L. Mandel, Fluctuations of Photon Beams: The Distribution of the Photo-Electrons, *Proc. Phys. Soc. (London)* **74**, 233 (1959).
- [199] L. Mandel, Intensity Fluctuations of Partially Polarized Light, *Proc. Phys. Soc. (London)* **81**, 1104 (1963).
- [200] L. Landweber, An Iteration Formula for Fredholm Integral Equations of the First Kind, *Amer. J. Math.* **73**, 615 (1951).
- [201] M. Bertero and P. Boccacci, *Introduction to Inverse Problems in Imaging* (IoP Publishing, Bristol and Philadelphia, 1998).
- [202] R. C. Aster, B. Borchers, and C. H. Thurber, *Parameter Estimation and Inverse Problems* (Elsevier, Amsterdam, 2013).
- [203] T. Kiesel, W. Vogel, V. Parigi, A. Zavatta, and M. Bellini, Experimental determination of a nonclassical Glauber-Sudarshan P function, *Phys. Rev. A* **78**, 021804(R) (2008).
- [204] A. Cabello, Violating Bells Inequality Beyond Cirel'son's Bound, *Phys. Rev. Lett.* **88**, 060403 (2002).
- [205] A. Cabello, Two qubits of a W state violate Bell's inequality beyond Cirel'son's bound, *Phys. Rev. A* **66**, 042114 (2002).
- [206] D. S. Tasca, S. P. Walborn, F. Toscano, and P. H. Souto Ribeiro, Observation of tunable Popescu-Rohrlich correlations through postselection of a Gaussian state, *Phys. Rev. A* **80**, 030101(R) (2009).

- [207] Y.-A. Chen, T. Yang, A.-N. Zhang, Zh. Zhao, A. Cabello, and J.-W. Pan, Experimental Violation of Bell's Inequality beyond Tsirelson's Bound, *Phys. Rev. Lett.* **97**, 170408 (2006).
- [208] B. A. Dubrovin, A.T. Fomenko, and S.P. Novikov, *Modern Geometry – Methods and Applications* (Springer, Berlin-Heidelberg, 1982).
- [209] Ch. W. Misner, K. S. Thorne, and J. A. Wheeler, *Gravitation* (Princeton University Press, Princeton and Oxford, 2017).
- [210] P. Kómár, E. M. Kessler, M. Bishof, L. Jiang, A. S. Sørensen, J. Ye, and M. D. Lukin, A quantum network of clocks, *Nat. Physics* **10**, 582 (2014).
- [211] D. Gottesman, Th. Jennewein, and S. Croke, Longer-Baseline Telescopes Using Quantum Repeaters, *Phys. Rev. Lett.* **109**, 070503 (2012)
- [212] D. Rideout, Th. Jennewein, G. Amelino-Camelia, T. F. Demarie, B. L. Higgins, A. Kempf, A. Kent, R. Laflamme, and X. Ma, Fundamental quantum optics experiments conceivable with satellites reaching relativistic distances and velocities, *Class. Quantum Grav.* **29** 224011 (2012).
- [213] C. Sabín, Quantum detection of wormholes, *Sci. Rep.* **7**, 716 (2017).
- [214] A. Bassi, A. Großardt, H. Ulbricht, Gravitational Decoherence, *Class. Quantum Grav.* **34**, 193002 (2017).
- [215] K. J. Resch, M. Lindenthal, B. Blauensteiner, H. R. Böhm, A. Fedrizzi, C. Kurtsiefer, A. Poppel, T. Schmitt-Manderbach, M. Taraba, R. Ursin, P. Walther, H. Weier, H. Weinfurter, and A. Zeilinger, Distributing Entanglement and Single Photons Through an Intra-City, Free-Space Quantum Channel, *Opt. Express* **13**, 202 (2005).
- [216] M. J. Garcia-Martinez, N. Denisenko, D. Soto, D. Arroyo, A. B. Orue, and V. Fernandez, High-Speed Free-Space Quantum Key Distribution System for Urban Daylight Applications, *Appl. Opt.* **52**, 3311 (2013).
- [217] C. Peuntinger, B. Heim, Ch. Müller, Ch. Gabriel, Ch. Marquardt, and G. Leuchs, Distribution of Squeezed States Through an Atmospheric Channel, *Phys. Rev. Lett.* **113**, 060502 (2014).
- [218] M. Krenn, J. Handsteiner, M. Fink, R. Fickler, and A. Zeilinger, Twisted Photon Entanglement Through Turbulent Air Across Vienna, *Proc. Natl. Acad. Sci. U.S.A.*, **112**, 14197 (2015).
- [219] C. Croal, C. Peuntinger, B. Heim, I. Khan, Ch. Marquardt, G. Leuchs, P. Wallden, E. Anderson, and N. Korolkova, Free-Space Quantum Signatures Using Heterodyne Measurements, *Phys. Rev. Lett.* **117**, 100503 (2016).
- [220] H. Endo *et al.*, Free-Space Optical Channel Estimation for Physical Layer Security, *Optics Express* **24**, 8940 (2016).
- [221] T. Schmitt-Manderbach, H. Weier, M. Fürst, R. Ursin, F. Tiefenbacher, T. Scheidl, J. Perdigues, Z. Sodnik, Ch. Kurtsiefer, J. G. Rarity, A. Zeilinger, and H. Weinfurter, Experimental Demonstration of Free-Space Decoy-State Quantum Key Distribution over 144 km, *Phys. Rev. Lett.* **98**, 010504 (2007).
- [222] J. Yin *et al.*, Quantum Teleportation and Entanglement Distribution over 100-Kilometre Free-Space Channels, *Nature* **488**, 185 (2012).

- [223] I. Capraro, A. Tomaello, A. Dall’Arche, F. Gerlin, R. Ursin, G. Vallone, and P. Villoresi, Impact of Turbulence in Long Range Quantum and Classical Communications, *Phys. Rev. Lett.* **109**, 200502 (2012).
- [224] T. Herbst, T. Scheidl, M. Fink, J. Handsteiner, B. Wittmann, R. Ursin, and A. Zeilinger, Teleportation of Entanglement over 143 km, *Proc. Natl. Acad. Sci. U.S.A.* **112**, 14202 (2015).
- [225] J.-Y. Wang *et al.*, Direct and Full-Scale Experimental Verifications Towards Ground-Satellite Quantum Key Distribution, *Nature (London)* **7**, 387 (2013).
- [226] J.-P. Bourgoin *et al.*, A Comprehensive Design and Performance Analysis of Low Earth Orbit Satellite Quantum Communication, *New J. Phys.* **15**, 023006 (2013).
- [227] G. Vallone, D. Bacco, D. Dequal, S. Gaiarin, V. Luceri, G. Bianco, and P. Villoresi, Experimental Satellite Quantum Communications, *Phys. Rev. Lett.* **115**, 040502 (2015).
- [228] G. Vallone, D. Dequal, M. Tomasin, F. Vedovato, M. Schiavon, V. Luceri, G. Bianco, and P. Villoresi, Interference at the Single Photon Level Along Satellite-Ground Channels, *Phys. Rev. Lett.* **116**, 253601 (2016).
- [229] D. Dequal, G. Vallone, D. Bacco, S. Gaiarin, V. Luceri, G. Bianco, and P. Villoresi, Experimental single-photon exchange along a space link of 7000 km, *Phys. Rev. A* **93**, 010301(R) (2016).
- [230] Zh. Tang, R. Chandrasekara, Y. Ch. Tan, C. Cheng, L. Sha, G. Ch. Hiang, D. K.L. Oi, and A. Ling, Generation and Analysis of Correlated Pairs of Photons aboard a Nanosatellite, *Phys. Rev. Applied* **5**, 054022 (2016).
- [231] K. Günthner *et al.*, Quantum-Limited Measurements of Optical Signals from a Geostationary Satellite, *Optica* **4**, 611 (2017).
- [232] S.-K. Liao *et al.*, Long-Distance Free-Space Quantum Key Distribution in Daylight Towards Inter-Satellite Communication, *Nat. Photonics* **11**, 509 (2017).
- [233] J.-G. Ren *et al.*, Ground-to-Satellite Quantum Teleportation, *Nature* **549** 70 (2017).
- [234] H. Takenaka, A. Carrasco-Casado, M. Fujiwara, M. Kitamura, M. Sasaki, and M. Toyoshima, Satellite-to-Ground Quantum-Limited Communication Using a 50-kg-Class Micro-Satellite, *Nat. Photonics* **11**, 502 (2017).
- [235] S.-K. Liao *et al.*, Space-to-Ground Quantum Key Distribution Using a Small-Sized Payload on Tiangong-2 Space Lab, *Chin. Phys. Lett.* **34**, 090302 (2017).
- [236] S.-K. Liao *et al.*, Satellite-to-ground quantum key distribution, *Nature* **549**, 43 (2017).
- [237] V. Tatarskii, *Effects of the Turbulent Atmosphere on Wave Propagation* (IPST, Jerusalem, 1972).
- [238] A. Ishimaru, *Wave Propagation and Scattering in Random Media*, (Academic Press, San Diego, 1978).
- [239] L. Andrews, R. Phillips, and C. Hopfen, *Laser Beam Scintillation with Applications*, (SPIE Press, Washington, 2001).
- [240] L. Andrews and R. Phillips, *Laser Beam Propagation through Random Media*, (SPIE Press, Washington, 2005).

- [241] R. L. Fante, Electromagnetic beam propagation in turbulent media, Proc. IEEE **63**, 1669 (1975).
- [242] R. L. Fante, Electromagnetic beam propagation in turbulent media: An update, Proc. IEEE **68**, 1424 (1980).
- [243] S. T. Hong and A. Ishimaru, Two-Frequency Coherence Function, Coherence Bandwidth, and Coherence Time of Millimeter and Optical Waves in Rain, Fog, and Turbulence, Radio Sci. **11**, 551 (1976).
- [244] C. H. Liu and K.C. Yeh, Propagation of Pulsed Beam Waves through Turbulence, Cloud, Rain, or Fog, J. Opt. Soc. Am. **67**, 1261 (1977).
- [245] A. Deepak, U. O. Farrukh, and A. Zardecki, Significance of Higher-Order Multiple Scattering for Laser Beam Propagation through Hazes, Fogs, and Clouds, Appl. Opt. **21**, 439 (1982).
- [246] M. Grabner and V. Kvicera, Multiple Scattering in Rain and Fog on Free-Space Optical Link, J. Lightwave Technol. **32**, 513 (2013).
- [247] I. P. Lukin, Random Displacements of Optical Beams in an Aerosol Atmosphere, Radiophys. Quantum Electron. **24**, 95 (1981).
- [248] H. T. Yura, K. G. Barthel, and W. Büchtemann, Rainfall-induced Optical Phase Fluctuations in the Atmosphere, J. Opt. Soc. Am. **73**, 1574 (1983).
- [249] I. P. Lukin, D. S. Rychkov, A. V. Falits, L. K. Seng, and L. M. Rong, A Phase Screen Model for Simulating Numerically the Propagation of a Laser Beam in Rain, Quantum Electron. **39**, 863 (2009).
- [250] A. Ishimaru, Theory and Application of Wave Propagation and Scattering in Random Media, Proc. IEEE **65**, 1030 (1977).
- [251] H. C. van de Hulst, *Light Scattering by Small Particles*, (Dover Publications, New York, 1981).
- [252] P. Diamant and M. C. Teich, Photodetection of Low-Level Radiation through the Turbulent Atmosphere, J. Opt. Soc. Am. **60**, 1489 (1970).
- [253] J. Peřina, On the Photon Counting Statistics of Light Passing through an Inhomogeneous Random Medium, Czech. J. Phys. **22**, 1075 (1972).
- [254] J. Peřina, V. Peřinová, M. C. Teich, and P. Diamant, Two Descriptions for the Photocounting Detection of Radiation Passed through a Random Medium: A Comparison for the Turbulent Atmosphere, Phys. Rev. A **7**, 1732 (1973).
- [255] P. Milonni, J. Carter, Ch. Peterson, and R. Hughes, Effects of Propagation through Atmospheric Turbulence on Photon Statistics, J. Opt. B **6**, S742 (2004).
- [256] G. P. Berman and A. A. Chumak, Photon distribution function for long-distance propagation of partially coherent beams through the turbulent atmosphere, Phys. Rev. A **74**, 013805 (2006).
- [257] G. P. Berman; A. A. Chumak, Quantum effects of a partially coherent beam propagating through the atmosphere, Proc. of SPIE, 6710 (2007).
- [258] G. P. Berman, A. A. Chumak, and V. N. Gorshkov, Beam Wandering in the Atmosphere: The Effect of Partial Coherence, Phys. Rev. E **76**, 056606 (2007).

- [259] G. P. Berman and A. A. Chumak, Influence of phase-diffuser dynamics on scintillations of laser radiation in Earth's atmosphere: Long-distance propagation, *Phys. Rev. A* **79**, 063848 (2009).
- [260] O. O. Chumak and R. A. Baskov, Strong Enhancing Effect of Correlations of Photon Trajectories on Laser Beam Scintillations, *Phys. Rev. A* **93**, 033821 (2016).
- [261] R. A. Baskov, O. O. Chumak, Boltzman-Langevin equation for laser beam propagation in turbulent atmosphere: scintillations for weak and moderate turbulence, arXiv:1712.04780v2[quant-ph].
- [262] C. Paterson, Atmospheric Turbulence and Orbital Angular Momentum of Single Photons for Optical Communication, *Phys. Rev. Lett.* **94**, 153901 (2005).
- [263] G. Vallone, V. D'Ambrosio, A. Sponselli, S. Slussarenko, L. Marrucci, F. Sciarrino, and P. Villoresi, Free-Space Quantum Key Distribution by Rotation-Invariant Twisted Photons, *Phys. Rev. Lett.* **113**, 060503 (2014).
- [264] H. Avetisyan and C. H. Monken, Higher order correlation beams in atmosphere under strong turbulence conditions, *Opt. Express* **24**, 2318 (2016).
- [265] Y. Zhang, Sh. Prabhakar, A. H. Ibrahim, F. S. Roux, A. Forbes, and Th. Konrad, Experimentally observed decay of high-dimensional entanglement through turbulence, *Phys. Rev. A* **94**, 032310 (2016).
- [266] N. Leonhard, G. Sorelli, V. N. Shatokhin, C. Reinlein, and A. Buchleitner, Entanglement protection by adaptive optics, *Phys. Rev. A*, in press (2018).
- [267] D. Elser, T. Bartley, B. Heim, C. Wittmann, D. Sych, and G. Leuchs, Feasibility of free space quantum key distribution with coherent polarization states, *New J. Phys.* **11**, 045014 (2009).
- [268] B. Heim, D. Elser, T. Bartley, M. Sabuncu, C. Wittmann, D. Sych, C. Marquardt, and G. Leuchs, Atmospheric channel characteristics for quantum communication with continuous polarization variables, *Appl. Phys. B* **98**, 635 (2010).
- [269] P. Ehrenfest, Bemerkung über die angenäherte Gültigkeit der klassischen Mechanik innerhalb der Quantenmechanik, *Z. Physik* **45**, 455 (1927).
- [270] V. P. Aksenov and V. L. Mironov, Phase Approximation of the Huygens-Kirchhoff Method in Problems of Reflections of Optical Waves in the Turbulent Atmosphere, *J. Opt. Soc. Am.*, **69**, 1609 (1979).
- [271] V. A. Banakh and V. L. Mironov, Phase Approximation of the Huygens-Kirchhoff Method in Problems of Space-Limited Optical-Beam Propagation in Turbulent Atmosphere, *Opt. Lett.* **4**, 259 (1979).
- [272] V. L. Mironov and V. V. Nosov, On the Theory of Spatially Limited Light Beam Displacement in a Randomly Inhomogeneous Medium, *J. Opt. Soc. Am* **67**, 1073 (1977).
- [273] V. L. Mironov, *Laser Beam Propagation in the Turbulent Atmosphere*, (Nauka, Novosibirsk, 1981) [in Russian].
- [274] R. Esposito, Power scintillations due to the wandering of the laser beam, *Proc. IEEE* **55**, 1533 (1967).
- [275] V. C. Usenko, B. Heim, C. Peuntinger, C. Wittmann, C. Marquardt, G. Leuchs, and R. Filip, Entanglement of Gaussian states and the applicability to quantum key distribution over fading channels, *New J. Phys.* **14**, 093048 (2012).



- [276] N. Hosseinidehaj and R. Malaney, Gaussian Entanglement Distribution via Satellites, *Phys. Rev. A* **91**, 022304 (2015).
- [277] F. A. S. Barbosa, A. J. de Faria, A. S. Coelho, K. N. Cassemiro, A. S. Villar, P. Nussenzweig, and M. Martinelli, Disentanglement in bipartite continuous-variable systems, *Phys. Rev. A* **84**, 052330 (2011).
- [278] S. N. Filippov and M. Ziman, Entanglement sensitivity to signal attenuation and amplification, *Phys. Rev. A* **90**, 010301(R) (2014).
- [279] M. Hillery, Amplitude-squared squeezing of the electromagnetic field, *Phys. Rev. A* **36**, 3796 (1987).
- [280] R. M. Gomes, A. Salles, F. Toscano, P. H. Souto Ribeiro, and S. P. Walborn, Quantum entanglement beyond Gaussian criteria, *PNAS* **106** 21517 (2009).



# Publications

## List of publications

- [I] A. A. Semenov, D. Yu. Vasylyev, W. Vogel, M. Khanbekyan, and D.-G. Welsch, Leaky cavities with unwanted noise, *Phys. Rev. A* **74**, 033803 (2006).  
DOI: 10.1103/PhysRevA.74.033803
- [II] A. A. Semenov, D. Yu. Vasylyev, W. Vogel, M. Khanbekyan, and D.-G. Welsch, Characterization of unwanted noise in realistic cavities, *Optics and Spectroscopy* **103**, 245 (2007).  
DOI: 10.1134/S0030400X07080139
- [III] M. Khanbekyan, D.-G. Welsch, A. A. Semenov, and W. Vogel, Quantum-state input-output relations for absorbing cavities, *J. Opt. B: Quantum Semiclass. Opt.* **7**, S689 (2005).  
DOI: 10.1088/1464-4266/7/12/035
- [IV] M. Khanbekyan, L. Knöll, D.-G. Welsch, A. A. Semenov, and W. Vogel, QED of lossy cavities: Operator and quantum-state input-output relations, *Phys. Rev. A* **72**, 05813 (2005).  
DOI: 10.1103/PhysRevA.72.053813
- [V] M. Khanbekyan, L. Knöll, A. A. Semenov, W. Vogel, and D.-G. Welsch, Quantum-state extraction from high-Q cavities, *Phys. Rev. A* **69**, 043807 (2004).  
DOI: 10.1103/PhysRevA.69.043807
- [VI] A. A. Semenov, W. Vogel, M. Khanbekyan, and D.-G. Welsch, Determination of quantum-noise parameters of realistic cavities, *Phys. Rev. A* **75**, 013807 (2007).  
DOI: 10.1103/PhysRevA.75.013807
- [VII] A. A. Semenov, A. V. Turchin, and H. V. Gomonay, Detection of quantum light in the presence of noise, *Phys. Rev. A* **78**, 055803 (2008).  
DOI: 10.1103/PhysRevA.78.055803
- [VIII] A. A. Semenov, D. Yu. Vasylyev, and B. I. Lev, Nonclassicality of noisy quantum states, *J. Phys. B: At. Mol. Opt. Phys.* **39**, 905 (2006).  
DOI: 10.1088/0953-4075/39/4/014
- [IX] V. N. Starkov, A. A. Semenov, and H. V. Gomonay, Numerical reconstruction of photon-number statistics from photocounting statistics: Regularization of an ill-posed problem, *Phys. Rev. A* **80**, 013813 (2009).  
DOI: 10.1103/PhysRevA.80.013813
- [X] A. A. Semenov and W. Vogel, Fake violations of the quantum Bell-parameter bound, *Phys. Rev. A* **83**, 032119 (2011).  
DOI: 10.1103/PhysRevA.83.032119
- [XI] A. A. Semenov and W. Vogel, Quantum light in the turbulent atmosphere, *Phys. Rev. A* **80**, 021802(R) (2009).  
DOI: 10.1103/PhysRevA.80.021802
- [XII] D. Yu. Vasylyev, A. A. Semenov, and W. Vogel, Toward global quantum communication: beam wandering preserves nonclassicality, *Phys. Rev. Lett.* **108**, 220501 (2012).  
DOI: 10.1103/PhysRevLett.108.220501

- [XIII] D. Yu. Vasylyev, A. A. Semenov, and W. Vogel, Quantum channels with beam wandering: an analysis of the Marcum Q-function, *Phys. Scr.* **T153**, 014062 (2013). DOI: 10.1088/0031-8949/2013/T153/014062
- [XIV] D. Vasylyev, A. A. Semenov, and W. Vogel, Atmospheric quantum channels with weak and strong turbulence, *Phys. Rev. Lett.* **117**, 090501 (2016). DOI: 10.1103/PhysRevLett.117.090501
- [XV] D. Vasylyev, A. A. Semenov, W. Vogel, K. Günthner, A. Thurn, Ö. Bayraktar, and Ch. Marquardt, Free-space quantum links under diverse weather conditions, *Phys. Rev. A* **96**, 043856 (2017). DOI: 10.1103/PhysRevA.96.043856
- [XVI] A. A. Semenov and W. Vogel, Entanglement transfer through the turbulent atmosphere, *Phys. Rev. A* **81**, 023835 (2010). DOI: 10.1103/PhysRevA.81.023835
- [XVII] M. O. Gumberidze, A. A. Semenov, D. Vasylyev, and W. Vogel, Bell nonlocality in the turbulent atmosphere, *Phys. Rev. A* **94**, 053801 (2016). DOI: 10.1103/PhysRevA.94.053801
- [XVIII] A. A. Semenov, F. Töppel, D. Yu. Vasylyev, H. V. Gomonay, and W. Vogel, Homodyne detection for atmosphere channels, *Phys. Rev. A* **85**, 013826 (2012). DOI: 10.1103/PhysRevA.85.013826
- [XIX] M. Bohmann, A. A. Semenov, J. Sperling, and W. Vogel, Gaussian entanglement in the turbulent atmosphere, *Phys. Rev. A* **94**, 010302(R) (2016). DOI: 10.1103/PhysRevA.94.010302
- [XX] M. Bohmann, J. Sperling, A. A. Semenov, and W. Vogel, Higher-order nonclassical effects in fluctuating-loss channels, *Phys. Rev. A* **95**, 012324 (2017). DOI: 10.1103/PhysRevA.95.012324

## Preprints

- [XXI] O. P. Kovalenko, J. Sperling, W. Vogel, and A. A. Semenov, Geometry of photocounting, arXiv:1801.02677 [quant-ph] (2018) <sup>8</sup>.

---

<sup>8</sup>The preprint with small editorial changes has been published 28 February 2018; see O. P. Kovalenko, J. Sperling, W. Vogel, and A. A. Semenov, Geometrical picture of photocounting measurements, *Phys. Rev. A* **97**, 023845 (2018). DOI: 10.1103/PhysRevA.97.023845